Nano Research
2022, 15(2): 787–804

ISSN 1998-0124 CN 11-5974/O4
https://doi.org/10.1007/s12274-021-3593-7

Review Article

Electrospinning nanofibers to 1D, 2D, and 3D scaffolds and their biomedical applications

Huiling Zhong[1,2,§], Jun Huang[2,§], Jun Wu[1,2] (✉), and Jianhang Du[1,3] (✉)

[1] *Guangdong Innovative Engineering and Technology Research Center for Assisted Circulation, the Eighth Affiliated Hospital of Sun Yat-sen University, Shenzhen 518033, China*
[2] *Key Laboratory of Sensing Technology and Biomedical Instrument of Guangdong Province, School of Biomedical Engineering, Sun Yat-sen University, Guangzhou 510006, China*
[3] *NHC Key Laboratory of Assisted Circulation (Sun Yat-sen University), Guangzhou 510080, China*
[§] *Huiling Zhong and Jun Huang contributed equally to this work.*

Received: 27 March 2021 / **Revised:** 9 May 2021 / **Accepted:** 12 May 2021

ABSTRACT

Electrospinning is a popular and effective method of producing porous nanofibers with a large surface area, superior physical and chemical properties, and a controllable pore size. Owing to these properties, electrospun nanofibers can mimic the extracellular matrix and some human tissue structures, based on the fiber configuration. Consequently, the application of electrospun nanofibers as biomaterials, varying from two-dimensional (2D) wound dressings to three-dimensional (3D) tissue engineering scaffolds, has increased rapidly in recent years. Nanofibers can either be uniform fiber strands or coaxial drug carriers, and their overall structure varies from random mesh-like mats to aligned or gradient scaffolds. In addition, the pore size of the fibers can be adjusted or the fibers can be loaded with disparate medicines to provide different functions. This review discusses the various structures and applications of 2D fiber mats and 3D nanofibrous scaffolds made up of different one-dimensional (1D) fibers in tissue engineering. In particular, we focus on the improvements made in recent years, especially in the fields of wound healing, angiogenesis, and tissue regeneration.

KEYWORDS

electrospinning nanofibers, structures, three-dimensional (3D) scaffolds, tissue engineering

1 Introduction

Electrospinning is commonly used in tissue engineering (TE), as the associated electrostatic spinning apparatus can form and expand continuous nanoscale fibers using a wide range of polymers and natural macromolecule solutions or melt [1]. Nanofiber formation through electrospinning is based on the uniaxial stretching of a viscoelastic solution due to electrostatic forces [2]. To realize this process, a high-voltage is applied to both the solution transmitter and the receptor to induce the formation of a liquid jet [3]. In general, an electrospinning apparatus consists of three major parts: a high-voltage supply that generates the electrostatic force, a syringe that loads the spinning solution, and a collector that forms flat nanofiber films (Fig. 1). During the electrospinning process, charged droplets of the electrospinning solution form at the tip of the needle owing to the tension exerted by the voltage. When the electrostatic repulsive force of the droplet exceeds the surface tension of the liquid, the droplet becomes conical in shape, and is referred to as a Taylor cone. The conical droplet is stretched into a thin jet by an electric field as the solvent gradually evaporates. Finally, the jet solidifies and is deposited on the collector, resulting in a random array of nanofibers [4].

One of the major advantages of electrospinning is its ability to generate fibrous structures similar to those of the extracellular matrix (ECM). The ECM is secreted by cells and is a three-dimensional (3D) fibrous network consisting of various proteins and proteoglycans. In addition to providing structural support to cells, it regulates cell attachment, diffusion, migration, and differentiation. Fibers are the basic structural components of several soft tissues. Human tissues are constituted by the inclusion of collagen fibers in the ECM. In addition to maintaining the structural integrity of the tissue, fibers can impart anisotropic and depth-dependent mechanical properties to tissues, with different orientation and density gradients [5, 6]. Tissue engineering involves the creation of scaffold materials to modulate cellular behavior by providing a suitable microenvironment that mimics the ECM [7]. The preparation of suitable tissue engineering materials to direct specific cell behaviors is an important area of research for

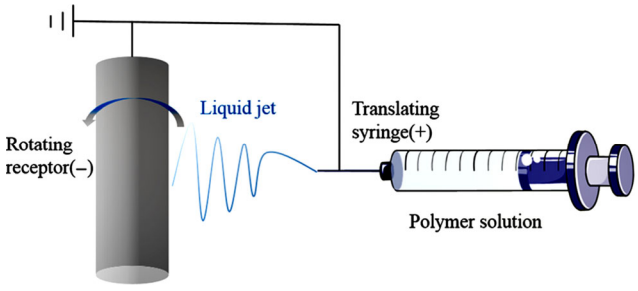

Figure 1 Schematic diagram of conventional electrospinning apparatus.

Address correspondence to Jun Wu, jw384@cornell.edu; Jianhang Du, dujh8@mail.sysu.edu.cn

biomaterial scientists. In addition to being used as medical devices and tissue scaffolds, biomaterials can be used to build platforms to study fundamental biological phenomena. In general, basic material properties such as the chemical composition, mechanical strength, surface morphology, and 3Dstructure can influence a wide range of cell behaviors, including adhesion, proliferation, migration, gene expression, and differentiation [8]. Owing to its high operability and efficiency, electrospinning can be used to fabricate porous nanofibers that enable cells to adhere to scaffolds, making it a versatile and promising fabrication method in the field of tissue engineering. Nonwoven nanoscale fiber mats produced by electrospinning have high surface-to-volume ratios, complex porous structures, excellent pore interconnections, and a variety of fiber morphologies [9]. Thus, electrospinning has several desirable properties for advanced biomedical applications, such as drug and bioactive factor encapsulation and delivery, cellular scaffolds, vascular scaffolds, wound healing dressings, tissue substitutes, etc.

Surface morphology of electrospun nanofiber-based scaffolds, including the diameter, orientation, and surface roughness of individual fibers, and the pore size, porosity, and surface pattern of the scaffold, plays a pivotal role in regulating cell behavior and tissue regeneration [7]. Moreover, these parameters also affect the biocompatibility, biodegradability, and mechanical properties of the scaffolds. Therefore, in this review, we systematically present different electrospun fiber structures, and analyze their morphologies, fabrication methods, and corresponding applications.

2 Micro-nano structure of one-dimensional (1D) electrospun fibers

There is no agreement in the literature on the definition of 1D nanofibers, and they can be nanofiber fragments, nanowires or single fibers [10, 11]. In this review a single fiber is hereby designated as a 1D structure and we will mainly introduce the different morphology that a single fiber can have.

2.1 Homogeneous nanofibers

Homogeneous nanofibers that have a smooth surface and uniform cross section are the most basic kind of electrospun fibers, and are convenient and easy to form [12]. A variety of water solutions or organo-soluble polymers and biomacromolecules, especially those with good biocompatible and biodegradable properties, such as polyvinyl alcohol (PVA), polycaprolactone (PCL), and gelatin, can be used as spinning solutions. Homogeneous nanofibers can be fabricated using either single or hybrid solutions, and the latter is generally used to achieve better functionality. For example, collagen has numerous advantages such as its biological origin and excellent biocompatibility and biodegradability, whereas chitosan has excellent antibacterial and anticorrosion properties. Chen et al. successfully used a collagen–chitosan complex to fabricate a smooth nanofiber membrane that could be applied as a biomedical scaffold [13]. In addition to using a combination of different solutions, attempts have been made to mix various solutions with drugs, with the aim of delivering drugs *in vivo*, which has led to the fabrication of various uniform nanofibers. For instance, Li et al. encapsulated finasteride (FNS) into PVA nanofibers using a co-electrospinning technique. The resulting nanofibers had a smooth surface and uniform diameter without forming beads on a string, indicating that FNS was well-dispersed in the PVA nanofibers without any obvious aggregation [14].

There are special cases. If the spinning fluid has a high viscosity, the electrostatic force will stretch the solution into a large diameter jet. Consequently, jet curing does not occur synchronously, forming a solid shell with a liquid core inside the fiber. As the solvent evaporates, the volume of the core shrinks and the shell collapses, resulting in ribbon fibers [15].

2.2 Coaxial nanofibers

Coaxial electrospinning (co-electrospinning) of core–shell (Fig. 2(e)), hollow (Fig. 2(f)), and multichannel (Figs. 2(a)–2(d)) nanofiber structures is a derived nanotechnology that improves upon conventional electrospinning [16]. Coaxial fibers have complex internal structures, unique anisotropies, and large specific surface areas; therefore, they have a high transmission efficiency. As they can be used to achieve controlled drug release, coaxial nanofibers have become widely popular in fields such as biotechnology and drug delivery [16, 17].

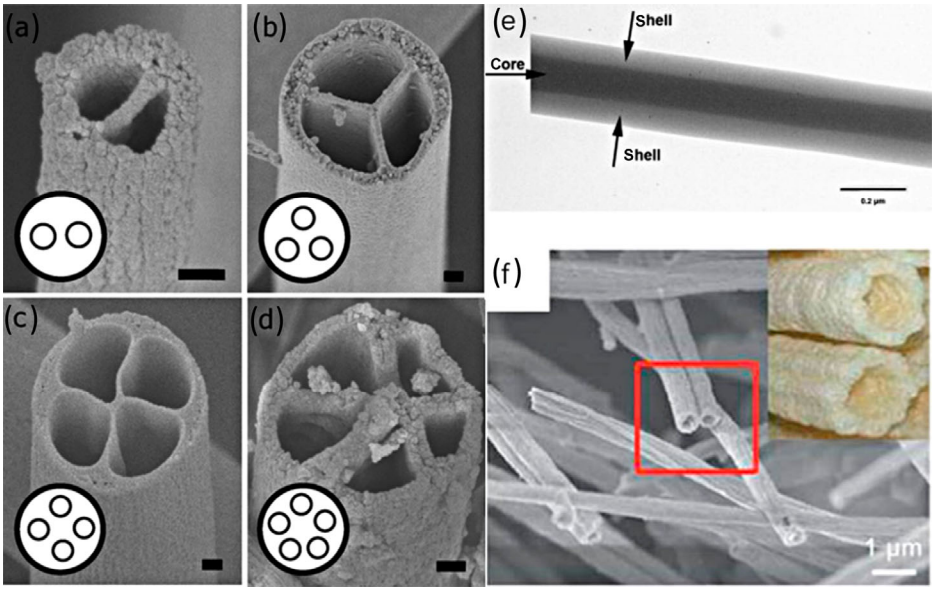

Figure 2 (a)–(d) Multichannel fibers (reproduced with permission from Ref. [18], © American Chemical Society 2007). (e) Solid coaxial fiber (reproduced with permission from Ref. [19], © Acta Materialia Inc. 2010). (f) Hollow fiber (reproduced with permission from Ref. [20], © Royal Society of Chemistry 2013).

Core–shell fibers: In 2003, Sun et al. described the process of fabricating core–shell nanofibers using a spinneret composed of two coaxial capillaries that could simultaneously spin two polymer solutions into a single core–shell structure nanofiber [21]. The propelling velocity of the liquid in the core layer must be lower than that of the liquid in the shell layer; if not, the shell layer of the fiber becomes thick and the inner core becomes bent [22]. The thickness of the shell is an important factor that affects the drug release rate; the thicker the shell, the slower the drug release rate [23]. Core–shell fibers can also be produced using emulsion electrospinning technology, which uses only a common single-channel needle, as opposed to conventional coaxial electrospinning. Emulsion electrospinning is a convenient method of manufacturing core–shell fibers using water-in-oil (W/O) or oil-in-water (O/W) emulsions to directly wrap hydrophilic or hydrophobic compounds [24].To investigate the difference in the protein loading capacity of blended and coaxial nanofibers, Ji et al. fabricated PCL-based nanofibrous scaffolds with bovine serum albumin (BSA) using blend and coaxial electrospinning [19]. The coaxial electrospinning technique provided uniform fibers with a smooth morphology and core–shell structure, and homogeneous protein dispersal was observed throughout the core of the fibers. In contrast, the blended electrospun fibers had a bead-on-string morphology with uneven protein distribution. In addition, the coaxial fibers had a more sustained release rate than the blended fibers. Li et al. [25] successfully developed an implantable hierarchical structured fiber device with a time-programmed dual drug release system using the coaxial electrospinning method. By encapsulating disulfiram (DSF) in the shell and doxorubicin hydrochloride (DOX·HCl) in the core, this fiber device can be used to realize long-term drug release and kill residual breast tumor cells to prevent tumor recurrence and metastasis.

Some substances have a low viscosity or a high surface tension when dissolved; consequently, they cannot be directly used as electrospinning solutions. However, these substances can be blended with materials that have excellent fiber-forming characteristics to create entanglements and physical bonds, and make them electrospinnable. Coaxial electrospinning is an effective method of fabricating core–shell nanofibers that have a supportive shell that wraps around a difficult-to-spin solution core. The outer liquid is usually a polymer solution, whereas the inner precursor does not need to be one; it can be a non-Newtonian suspension of particles, or even a Newtonian liquid [26]. Chitosan is a favorable anti-bacterial material that has a wide range of applications in biomedicine. However, owing to its limited chemical properties, it cannot be easily fabricated into antibacterial membranes. Pakraven et al. used coaxial electrospinning to produce polyethylene oxide (PEO)–chitosan nanofibers with a core–shell structure that are uniform in size and defect-free [27]. A new triaxial electrospinning process was developed wherein the outer solution is a non-spunnable solvent mixture, the intermediate fluid is a non-spunnable dilute polymer solution, and only the inner fluid is electrospinnable [28]. The thickness of the shell can be precisely controlled by the flow rate of the intermediate fluid during electrospinning.

Hollow fibers: Compared to solid nanofibers, hollow nanofibers have a larger surface area and higher aspect ratio, thus providing more active sites for ion adsorption, which improves the embedding of active species [29]. Hollow fibers can be fabricated through coaxial electrospinning using two different techniques [30]: core decomposition and core extraction. The former uses a solvent to dissolve the core material selectively while preserving the shell portion, whereas the latter removes the core material through heat treatment. The cores of coaxial nanofibers can be removed [31, 32].

Multi-channel fibers: Nanofibers with multi-channel structures can be fabricated by inserting multiple spinnerets into a needle. Some water-soluble materials, such as polyvinyl pyrrolidone (PVP) and polyethylene glycol (PEG), are commonly used as core materials [33]. The cores can either be retained as voids or filled with functional materials. Hollow and multichannel fibers have been widely studied in the fields of microelectronics, sensors, and battery energy [20, 29, 30]; however, their applications in biomedicine are still few. Two immiscible polymers and a sacrificial ferritin template were used to synthesize nanoscale SnO_2 multichannel nanofibers loaded with a PtO_2 catalyst; the resulting PtO_2–SnO_2 fibers showed excellent response to acetone gas [34].

2.3 Bead-on-string nanofibers

Nanofibers are not always uniform in diameter. In some cases, they have a bead-on-string morphology that can be attributed to insufficient stretching of the filaments during the whipping of the jet by the surface tension variations [35]. Variations in the electrospinning parameters can lead to numerous variations in the physical and chemical properties of electrospun materials. Various factors such as the applied voltage, viscoelasticity of the solution, selected solvent system, solute concentrations, salt additives, charge density, and surface tension of the solution, can affect the occurrence of beads. In particular, solution concentration plays a fundamental and practical role in bead formation [36]. Furthermore, several methods can be used to adjust and control the shape and size of bead fibers, such as varying the electrode geometry, polymer solution feed rate, solvent system, environment humidity, and substrate form. Significant attention has been devoted to studying

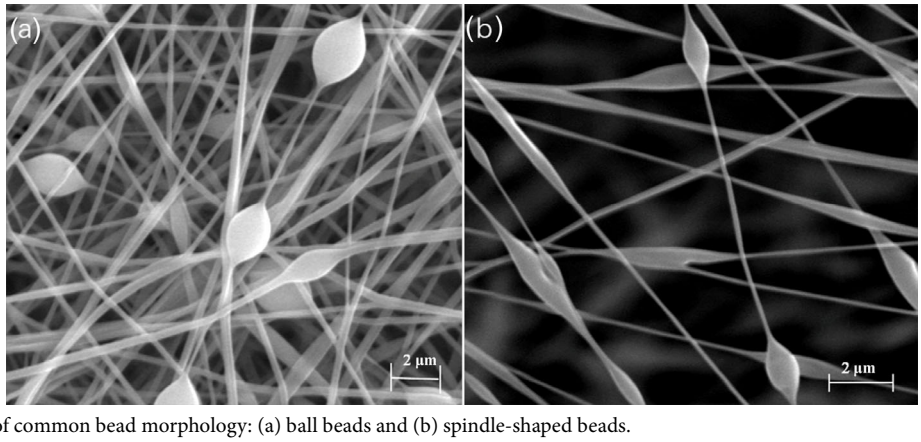

Figure 3 Two kinds of common bead morphology: (a) ball beads and (b) spindle-shaped beads.

the formation and morphology of beads in electrospun fibers [37–39]. For example, a combination of electrostatic spinning and electrospraying using a low viscosity coaxial jet fluid and a high viscosity spray lining fluid for the outer layers, was used to create bead-on-string heterostructured fibers (BSHFs) [40].

Initially, beads were considered to be a morphological defect, and several methods were used to avoid or eliminate this phenomenon. Subsequently, beaded fibers with a complete structure connected by fibers were found to provide more efficient controlled and sustained drug release [41], especially for micron drugs [42]. The drug encapsulation ability of bead-on-string fibers is directly related to the bead diameter, as it determines the depth at which the drug is embedded. In addition, the strength and toughness of the composite can be enhanced by the introduction of beaded fibers [43]. For example, beaded BSA-loaded nanofibers with core–shell structures can effectively support the attachment and proliferation of human mesenchymal stem cells (hMSCs) [44]. Considering the difference in the pH environments of cancer cells and normal cells, Xi et al. fabricated a pH-responsive coaxial beaded fiber loaded with DOX that releases less DOX when it encounters healthy tissue and more DOX when it encounters a tumor [45]. Therefore, coaxial bead fibers have significant potential for application in continuous drug delivery systems for cancer treatment.

2.4 Helical and twisted nanofibers

Helical structures are common in natural fibers. Owing to their unique properties, they have significant value in research and application. Helical structures are the basic configuration of several biological molecules, such as proteins, deoxyribonucleic acid (DNA), and starch. In addition, certain microorganisms, such as *Spirulina*, have spiral-shaped bodies [51]. In 2004, Kessick fabricated a microscale helical structure using electrospinning [52]. The microscale helical coils were fabricated using a complex of PEO and poly(aniline sulfonic acid) (PEO/PASA), and differed considerably from other common fiber structures (Fig. 4(a)). He observed that the helical fibers were formed by the viscoelastic shrinkage of charged fibers after partial neutralization. Subsequently, Yu et al. prepared oriented helical PCL fibers on tilted slides using a novel setup [51], wherein the helical fibers were formed by jet distortion while impacting the receiver surface. The position and angle of inclination of the tilted slides played a decisive role in the formation of the helical structures. When fibers are less crimped, they form twisted fibers (Fig. 4(b)). Dabirian employed a modified electrospinning instrument with two oppositely charged nozzles to produce uniform, continuous, and strong twisted polyacrylonitrile (PAN) yarns [53].

Silva et al. reviewed the three main situations in which

Table 1 Parameters affecting bead formation

Influence factors	Parametric variation	Results
Applied voltage [46]	Low	The droplet is dominated by surface tension; several microbeads are formed that are almost spherical.
	Increase	The tensile effect of the electric field force gradually exceeds the effect of the surface tension; the number of beads decreases and their shape changes to a spindle shape.
	High	The beads decrease or even disappear; however, extremely high voltages lead to insufficient volatilization of the jet, which affects spinning stability, and may result in the formation of string beads.
Solution feed rate [40]	Increase	The tensile effect of the electric field becomes weak, and the instability of the jet flow becomes stronger. Consequently, the diameter of the fibers and the beads increases, which leads to an increase in the number of beads.
	Decrease	Beads are fewer in number and smaller in size, with fine fibers.
Working distance [47]	Decrease	Solvent volatilization is not timely; the fibers bond to each other easily and form beads or droplets.
	Increase	The electric field intensity is weak; the jet velocity and stability are affected, resulting in beaded or fused fibers.
Solution additives	Alcohol (C_2H_5OH)	The formation of beads is reduced.
	$CHCl_3$ [42]	Large beads are formed.
	Acetone [42]	Small beads are formed.
	N,N-dimethyl formamide (DMF) [46]	Bead size decreases.
Solution conductivity/ salt additives [39]	Low	The surface tension of the jet is relatively strong, which easily induces the formation of beads.
	High	The charge density on the jet surface is large, which enhances the tensile refinement effect; this is conducive to the formation of uniform and smooth fibers.
Solvent system [48]	—	Fast-evaporating solvents aid fiber formation, which in turn leads to beading. Solvents may also alter the conductivity and surface tension of the solution, which also affects the final fiber shape.
Polymer concentration [49]	Low	The degree of molecular entanglement and the viscous resistance of the solution are small; consequently, it cannot resist the stretching of the electrostatic field force and the repulsion of the electric charge. The jet breaks and forms discrete beads owing to the action of the surface tension.
	Increase	As the concentration increases, the viscoelastic force of the jet gradually increases; the fibers are attached with a string of beads.
	High	As the viscoelastic force increases, the number of beads gradually decreases and eventually disappears, forming smooth fibers.
Surfactant additives [50]	Cationic surfactants	Bead formation is prevented; increasing the concentration of the cationic surfactant leads to thinner fibers.
	Non-ionic surfactants	Although bead formation is not prevented, the number of beads reduces and the fiber morphology changes.
Relative humidity [40]	Increase	The beads swell as they absorb water and increase in volume.
	Decrease	The beads taper to form a spindle-shaped string of beads.

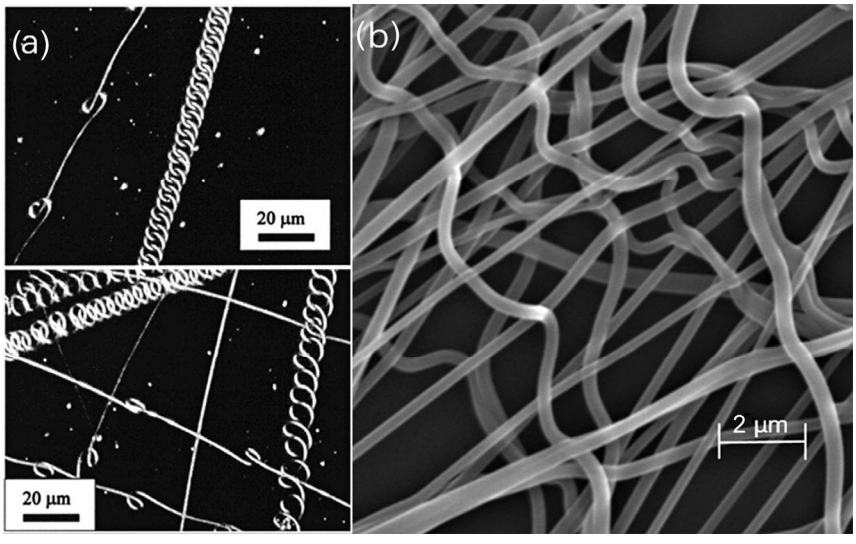

Figure 4 (a) Helical fibers electrospun using a complex of PEO/PASA (reproduced with permission from Ref. [52], © American Institute of Physics 2004). (b) PVA fiber curled under the action of a positive high voltage of 16 kV and a negative high voltage of 7 kV.

helical fibers are generated [54]: (1) large deformations that occur when the fibers impact the collector owing to the instability of the mechanical buckling; (2) the twisting motion of the fiber owing to an external mechanical or electric field; and (3) helical structures generated through asymmetric contractions owing to a mismatch of the elastic properties between the different regions of the fiber.

Twisted nanofibers have higher elasticity, making them suitable for use as synthetic collagen membranes. In addition, their structural properties can mimic those of double-stranded DNA or *Spirulina*. However, although the electrospinning method of preparing single helical nanofibers is relatively mature, significant improvements are required before they can be used for biomedical applications.

2.5 Nanofiber yarns

Owing to the whip and oscillation of the electrospinning jets and a lack of control over the electrostatic force, which controls the orientation and crystallization of fibers, randomly-oriented short fibers with isotropic structures in the form of nonwoven fiber mats can be produced [55]. According to the Halpin–Tsai equations [56], composites containing continuous fibers have better physical strength and mechanical properties than those containing short fibers. As the fiber length increases, the reinforcing effect also increases simultaneously, as the level of the plateau rises. Therefore, scientists prepare yarns with groovy strengths using continuous long fibers that have a high intensity. In 2003, Frank et al. employed an electrospinning apparatus to arrange single-walled carbon nanotubes (SWNTs) into a continuous nanoscale composite fibril. This improved the thermal stability and provided a significant reinforcement effect with less than 3% volume of the SWNT [57].

Conventionally, bundles of nanofiber yarns are prepared using an aligned fiber array, to obtain yarns with homogeneous thicknesses. Therefore, the fiber orientation can be controlled (this is discussed in the subsequent section). Liu et al. used an annular collector to prepare short fibrous yarns (420 mm) with diameters of 750–1000 nm through two-fold pre-drafting and twisting. The results indicated that this technique could be used to conveniently fabricate fibrous bundles and yarns [58]. In addition, ordinary nonwoven nanofiber membranes can be cut into long, thin strips and then twisted to produce yarn. The tensile strength and Young's modulus of the yarn can be improved by increasing the width of the nonwoven nanofiber mat and increasing the number of twists [59].

Researchers have devoted significant efforts towards exploring the potential applications of nanoyarns in biomedicine. Nanofiber bundles and yarn-based scaffolds have excellent cell infiltration rates compared to basic electrospun nonwoven fiber mats and can be incorporated into the larger field of post-processing technologies [60]. Wu et al. fabricated two nanoyarn scaffolds using dynamic liquid electrospinning and analyzed their effect on promoting cell growth, infiltration, and vascularization compared to traditional nanofiber scaffolds. The results indicated that the nanoyarn scaffolds are better [61, 62]. Antibiotics and other antimicrobial components can be added to the fibers, to use the yarn as antimicrobial surgical sutures [63]. Maleki et al. used electrospinning to manufacture continuously-twisted poly(L-lactic acid) (PLLA)/PVA blended yarns containing cefazolin, such that the drug can be released in a controlled manner over a long period of time to prevent implant infections.

3 Configurations of electrospun nanofibers

3.1 Randomly-oriented structures

Nanofibers deposited on the surface of a conductive plate or a rotating conductive drum present a randomly-oriented mess owing to the bending instability of the highly charged jet. Randomly-oriented nanofibers are deposited as a nonwoven mat, with a high porosity of around 50% to more than 90%. Consequently, they have one of the highest surface-to-volume ratios of all cohesive porous materials [64]. However, they have very small apertures, ranging from a few tenths of a nanometer to several micrometers in diameter [65, 66]. Generally, the pore diameter decreases with the increase in porosity. Such structures can be used to protect the surface of wounds while allowing air to permeate, and are often used as hydrogels in wound healing. In addition, these fiber membranes can be designed to accelerate esthetic wound repair owing to their capacity to absorb excess exudate and maintain a stable microenvironment that promotes epithelial regeneration [67]. In addition, they can be used for bone or cartilage applications that require a certain load-bearing capacity. Kumar sandwiched antibiotics into nanofiber mats and performed drug release tests that showed that 95% of the drug was released within 8 h [68],

which indicates that nanofibers loaded with antibiotics can be used as drug carriers.

3.2 Aligned nanofibers

Continuous, linearly-aligned yarns can be fabricated by replacing the traditional electrospun collector with bespoke collectors, speed-rotating collectors, or aligned pins. Figures 5(a)–5(c) show a modified setup using two parallel metal plates, with aligned PVP nanofibers formed on them [69]. Magnetic-field-assisted electrospinning (MFAES) (Fig. 5(d)) can be achieved by introducing two bar magnets at both ends of the collector to produce aligned straight or wavy fibers [70].

Zhang et al. reported that stable jet electrospinning (SJES) is an effective method of producing aligned fibers [71–73]. It does not require the use of complex collectors or electric field manipulations, and only involves the introduction of a small amount of ultra-high molecular weight PEO to prepare spinning solutions with excellent fiber-forming ability to restrain the bending instability of electrospinning, thereby forming long and stable jets. A novel method of producing a mass of aligned fibers is by using a centrifugal electrospinning (CES) spinneret system [74]. As the rotational speed of the spinneret increases, the orientation of the fibers also increases, and the fiber diameters decrease. Laser ablation can also be used to produce aligned nanofiber mats. In contrast to other aligned fiber production methods, laser ablation is used to carve aligned grooves into disordered fiber membranes. A femtosecond laser can be used to apply ultrashort laser pulses to the target material, minimizing thermal stress and collateral damage, and preventing the collapse of the fiber structure or a reduction in its mechanical stability [75, 76]. This technology can be used to create customizable patterns on fiber pads to achieve cell infiltration and control adherent cell morphology.

Some tissues, such as cartilage [77], tendons [78, 79], ligaments [78], blood vessels [73], nerve conduits [80, 81], etc., are composed of arranged fibers and directed cells.

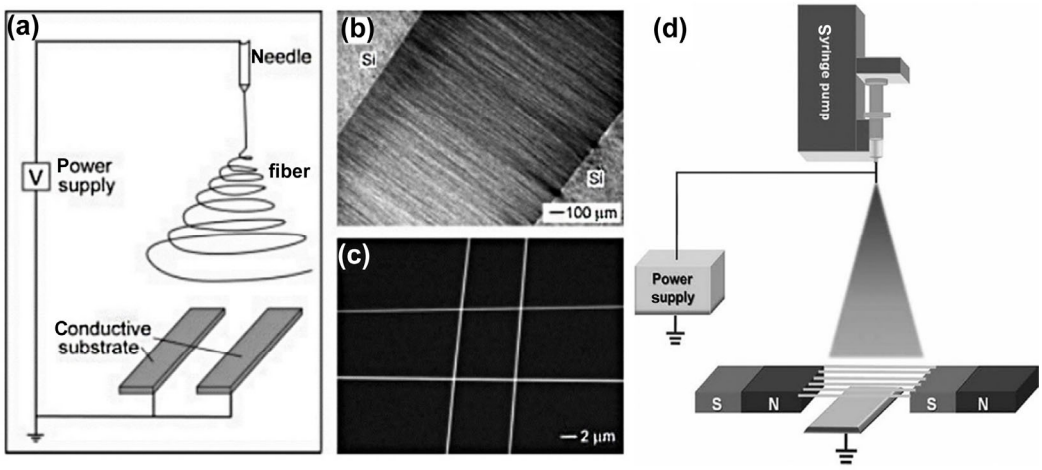

Figure 5 (a) Bespoke collector system and ((b) and (c)) aligned fibers produced using this collector system (reproduced with permission from Ref. [69], © WILEY-VCH Verlag 2004). (d) Magnetic-field-assisted electrospinning (reproduced with permission from Ref. [70], © WILEY-VCH Verlag 2010).

Table 2 Biomedical applications of aligned fibers

Polymers	Application field	Highlight
Chitosan-collagen/PLLA	Bionic scaffolds for flexor tendon regeneration	Offer a suitable structure for flexor tendon regeneration [79]
Poly(L-lactide-*co*-caprolactone)/poly(L-lactic acid) (PLCL/PLLA)	Adjustable stiffness of aligned fibrous scaffolds for regulation of vascular smooth muscle cells (SMCs)	Promotes the directional growth of vascular SMCs and human vascular endothelial cells (HUVECs) [73]
PVP	Drug release matrices	The fiber orientation, layer stacking, and patterns can control the release rate of antibiotics [74]
Alginate/PEO	Aligned cell-laden fibrous scaffolds	Facilitates myogenic differentiation and regenerates skeletal muscle tissue [82]
Polypyrrole (PPy) and PLLA	Aligned conductive nerve fibrous scaffolds	Regulates the alignment of cellular neurites along the direction of the fiber axis or electric potential [81]
Collagen/poly(ε-caprolactone) (PCL)	Radically aligned fibers with gradient of stromal-cell-derived factor-1α (SDF1α) to guide neural stem cells (NSCs)	Guides and enhances the migration activity of NSCs from the periphery to the center along an array of electrospun fibers [83]
PCL/PVP	Nerve guidance conduit with nanoscale grooves	Promotes neurite elongation and Schwann cell migration [84]
Nerve growth factor (NGF)/PCL	Nerve conduit for enhancing and directing sciatic nerve regeneration	A 15 mm gap was closed in a rat model of sciatic nerve defects, and axon regeneration and functional recovery were promoted [80]
GelMA	Hydrogel nanofibers for regeneration of spinal cord	Induces further differentiation of endogenous neural stem cells into neurons, and forms more synaptic connections with new functions; also inhibits the formation of a glial scar [85]
Poly(ε-caprolactone)-block-poly(2-aminoethyl ethylene phosphate) (PCL-PPEEA)	3D nanofibers-hydrogel scaffold for gene delivery	Provides continuous non-viral delivery of protein and nucleic acid therapy drugs, as well as collaborative contact guidance in the treatment of nerve injuries [86]

Disordered nanofibers cannot regulate the direction of cell growth and are not strong enough to mimic these structures. Aligned nanofibers can help regulate cell growth and better facilitate tissue repair.

3.3 Gradient fibrous scaffolds

Several types of fibrous scaffolds that have been developed do not match the required application. In some cases, the pore size is too small for the cell to adhere well, whereas in others, although the pore size is large enough, it lacks regularity. Consequently, the cell does not grow as vigorously as it would in a natural microenvironment. This is especially true for bionic human dermal applications as the human dermis is not homogeneous, but has a complex multi-layer structure. In addition, various gradient structures have also been found inside the human body, such as the interface between tissue-like cartilage and the dermis [87, 88]. Therefore, novel scaffolds with appropriate porosity and satisfactory gradient structures that can mimic the ECM are required to obtain more efficient biofunction. In particular, nanofibrous scaffolds with gradients, including density gradients, drug gradients, functional gradients, and double gradients, are an urgent requirement. The fabrication of such scaffolds requires the use of specialized techniques or equipment, such as melt electrospinning direct writing and 3D printing technology, to produce a suitable 3D gradient architecture.

Density gradients: The construction of gradient scaffold structures is primarily based on the integration of several layers with different pore sizes. Huang et al. combined multi-step electrospinning with low-temperature (LTE) collection and successfully constructed a 3D multi-layered silk fibroin scaffold with a gradient pore size [89]. They used a two-chamber box as the collector to vary the pore size of the nanofiber membranes, wherein one of the chambers was filled with liquid nitrogen. By changing the vertical order of the chambers and adjusting certain electrospinning parameters, medium pore layer (MPL) and large pore layer (LPL) scaffolds can be obtained as shown in Figs. 6(a) and 6(b). The scaffold, which is assembled with three layers of small, medium, and large pores, offers significant potential in the field of tissue repair as its gradient pore structure better mimics human interface tissue.

Drug gradients: In some cases, chemotactic fibers are required to direct the topological growth of nerves or tissues, and scaffolds with layered gradients are not necessary. Highly oriented fibers with drug-gradient-guided fibers are also suitable. For example, the fibers can be loaded with different concentration gradients of growth factors, and the nerve can be guided to expand along the axon [80, 83].

Functional gradients: Functional gradient nanofiber membranes can regulate the composition, structure, and biological activity of each layer, and have attracted significant attention in the field of biomedicine. He et al. [90] reported a functionally graded membrane consisting of two aligned surface layers of gelatin nanofibers and a randomly-oriented core layer of PCL nanofibers (Fig. 6(c)). This surface arrangement facilitates the migration and proliferation of osteoblasts, improves biocompatibility, and enhances bone regeneration; the inner layer provides isotropic mechanical strength to the membrane and has an antibacterial function due to the presence of antibiotics.

Double gradients: At the junction between different tissues, double-gradient scaffolds are required to connect the different tissues. Marco et al. designed and manufactured a novel functional gradient membrane consisting of a core layer and two functional surface layers [91]. The two surface layers were primarily composed of nano-hydroxyapatite (n-HAp) and metronidazole (MET), respectively, and were designed to be in contact with bone and epithelial tissues, respectively.

3.4 Large pore nanofiber membranes

Traditional electrospinning methods generally produce scaffolds with small pores, which can be applicable to skin wound repair

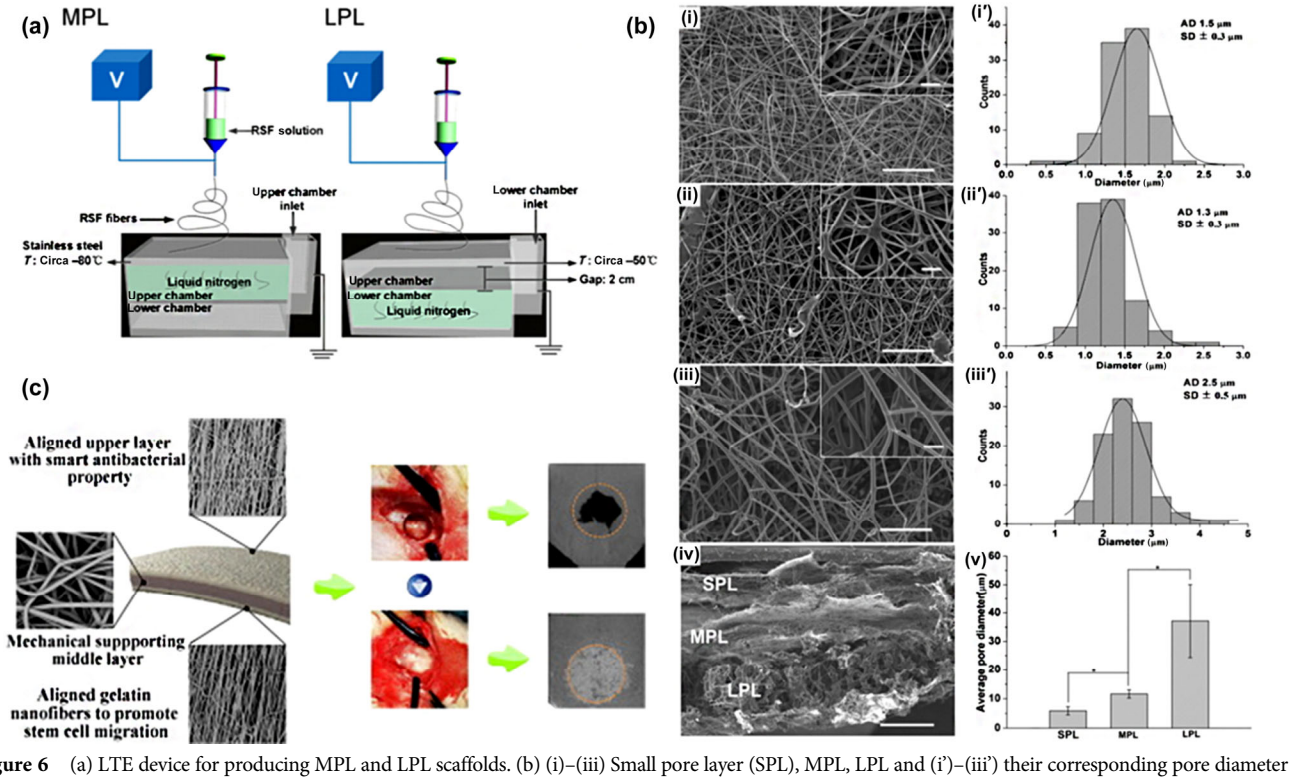

Figure 6 (a) LTE device for producing MPL and LPL scaffolds. (b) (i)–(iii) Small pore layer (SPL), MPL, LPL and (i')–(iii') their corresponding pore diameter distribution; (iv) cross section of the gradient pore scaffold; (v) average pore diameter of the three layers (reproduced with permission from Ref. [89], © Elsevier B.V. 2018). (c) Functionally graded scaffold for cartilage regeneration (reproduced with permission from Ref. [90], © Elsevier B.V. 2020).

dressing and dermis restructuring, where barrier protection is essential or cell infiltration is not necessary. However, small pores can limit cell migration, nutrient supply, and metabolic waste removal, whereas excessively large pores can have a negative effect on cell adhesion and intracellular signal expression. Consequently, scaffolds with a suitable pore size considering the corresponding application area are required. The 3D microenvironment and scaffold interconnectivity are also vital for cell movement and recombination [92]. Interconnections not only offer a template for cell adhesion and proliferation, but also facilitate the transport of nutrients and metabolites within and outside the engineered tissue. Although there is a lack of consensus on the optimal pore size for the effective growth of different cells or tissue repair, most researchers agree that a pore size of tens to hundreds of micrometers is required to provide sufficient space for cell ingrowth and diffusion [93, 94].

Table 3 Suitable pore sizes for different applications

Application	Suitable pore size
Skin regeneration	20–125 μm [95]
Chondrocyte ingrowth	> 7 μm [96]
Fibroblast binding	> 10 μm [89]
Osteogenesis differentiation	50 μm [97]
Liver tissue regeneration	45–145 μm
Vascular smooth muscle cell binding	60–150 μm [95]
Angiogenesis	200–300 μm
Bone regeneration	> 100 μm [98]
Osteocyte infiltration	~ 36 μm [99]

Large-pore scaffolds can be fabricated using the emulsion template method [100], gas forming, freeze drying, particulate leaching [101–103], etc. Typically, porous electrospun nanofibers can be prepared by selectively removing one component through phase separation and post-treatment [104] methods, such as particle leaching, improved collectors [105], micro-nano fiber deposition, physical post-processing, etc.

High-power ultrasound can promote fluid absorption in scaffolds, thereby resulting in a marked increase in the average pore size, pore interconnectivity, and porosity [106]. Ultrasound can also be used to promote cell infiltration by increasing the size of the scaffold [99]. However, the ultrasonic treatment process can lead to the loosening of the fiber connections and the opening of the internal structure of the scaffold, which reduces the mechanical strength of the scaffold owing to a reduction in the fiber density [107]. Particle leaching is also commonly used during electrospinning to create pores, but this method primarily produces porous structures on single fibers. Moreover, some limitations exist. For example, the improvement in cellular infiltration is insufficient as the increase in pore size is rather limited [108], which also decreases pore interconnectivity [109]. In addition, it is difficult to elute particles embedded at the depths of a scaffold. Compared to particulate leaching methods, low-temperature electrospinning, which is also known as cryogenic electrospinning (CE), offers better control over pore formation performance [110]. Ice crystals can be used as electrospinning collectors to create 3D scaffolds with large and interconnected pores. This technique was first proposed by Simonet et al. [111] and later developed by Leong et al. [112].

Moreover, melt electrospinning writing (MEW) technique, which we will discuss in detail in the next section, can be used to produce microfibers with large pores, and can be used in combination with particulate leaching [113] or solution electrospinning to fabricate scaffolds with a satisfactory pore size and porosity. Traditionally, polymers dissolved in a solvent were only electrospun into nanofibers. However, Mikos revealed that if the fibers are randomly deposited, they should be no less than 4 μm in diameter in order to manufacture a scaffold with an average pore diameter of at least 20 μm [114]. Using a highly viscous polymer melt instead of a solution with a lower viscosity can significantly improve the directional stability of the fiber [115], thereby enabling the formation of ordered patterns made up of straight fibers on the collector [116]. This technique can provide large-volume, highly-ordered, micrometer-scale scaffolds whose maximum height can exceed 7 mm [117].

4 3D structure of nanofibrous scaffolds

When electrospun nanofibers were first applied to human tissues, they were mostly in the form of two-dimensional (2D) nanofiber membranes, which are relatively easy to form using solutions that have high biocompatibility and suitable viscosity. Electrospinning has been widely used to produce 2D nonwoven fiber mats, which are generally used as wound dressings. In contrast, the applications of electrospun fibers for 3D tissue engineering scaffolds are limited. Compared to single-structure scaffolds, multi-layered scaffolds have better biomechanics, biocompatibility, biodegradability, etc.

Significant effort has been devoted to improving the bionic performance of electrospun fibers and fabricating 3D scaffolds using auxiliary equipment or modified electrospinning apparatuses. The most commonly used methods for manufacturing 3D electrospun scaffolds are the vertical stacking of nanofiber film layers [118, 119], incorporation of nanofibers into hydrogels [86], rolling of nanofiber mats into tubular structures [120], employing templates to assist with collection [121], and combining nanofibers with microfibers produced through 3D printing and melt electrospinning.

The layer-upon-layer stacking method is the most frequently used method for constructing 3D scaffolds. Park et al. developed a novel hybrid scaffold by stacking layers of aligned fibers and randomly-oriented fibers [119]. The upper part of the scaffold comprised an aligned fiber layer with a highly ordered structure that provides uniaxial topographic guidance, and the lower part of the scaffold comprised a random fiber layer that provides mechanical stability and support.

4.1 Technology to assist the preparation of 3D nanofibrous scaffolds

4.1.1 3D printing technology

Compared with electrospinning, 3D printing has the advantage of realizing controlled 3D model construction through computer-aided design (CAD) and layer printing [122]. It offers significant potential in realizing personalized biomedical devices and tissue engineering scaffolds. Manufacturing tissue-engineered scaffolds with adjustable shapes, suitable structures, and desirable mechanical properties is a significant challenge. Besides, it is not ideal to rely solely on a single technology, whether electrospinning or 3D printing. Chen et al. incorporated dispersed electrospun gelatin/polylactic lactic-glycolic acid (Gel-PLGA) fibers into a cartilage decellularized matrix ink for 3D printing [123]. The incorporation of the fibers not only improved the rigidity of the cartilage scaffold,

but also enhanced its toughness. Furthermore, the scaffold enhanced articular cartilage repair in rabbits both *in vitro* and *in vivo*. Chen et al. also obtained shape-deformation hydrogels with rapid deformation and enhanced 3D shape designability [124].

Eom et al. proposed an original hydrogel-assisted electrospinning process (GelES) using a hydrogel receiver in place of a traditional metal collector [125]. This technique enables the fabrication of various 3D nanofiber macrostructures with customizable complexity (Fig. 7). The use of 3D printing technology in the preparation of 3D hydrogels significantly increases the diversity of 3D nanofiber macrostructure designs. The advantages of hydrogels (e.g., high water retention and good biocompatibility) and nanofibers (e.g., high surface-to-volume ratio and high robustness) can be combined to build 3D hydrogel structures in the shape of any complex tissue defect. Therefore, it can be used as a high permeability barrier and applied to tissue defects to induce tissue regeneration.

Remarkably, 3D printing combined with electrospinning can completely encapsulate cells in the middle layer to realize cell functions. Lee et al. fabricated human adipose-derived stem cells (hASC) spheroids, wrapped them with a 3D-printed mesh structure, and added electrospun nanofiber membranes on the structure to create a scaffold that can maintain the

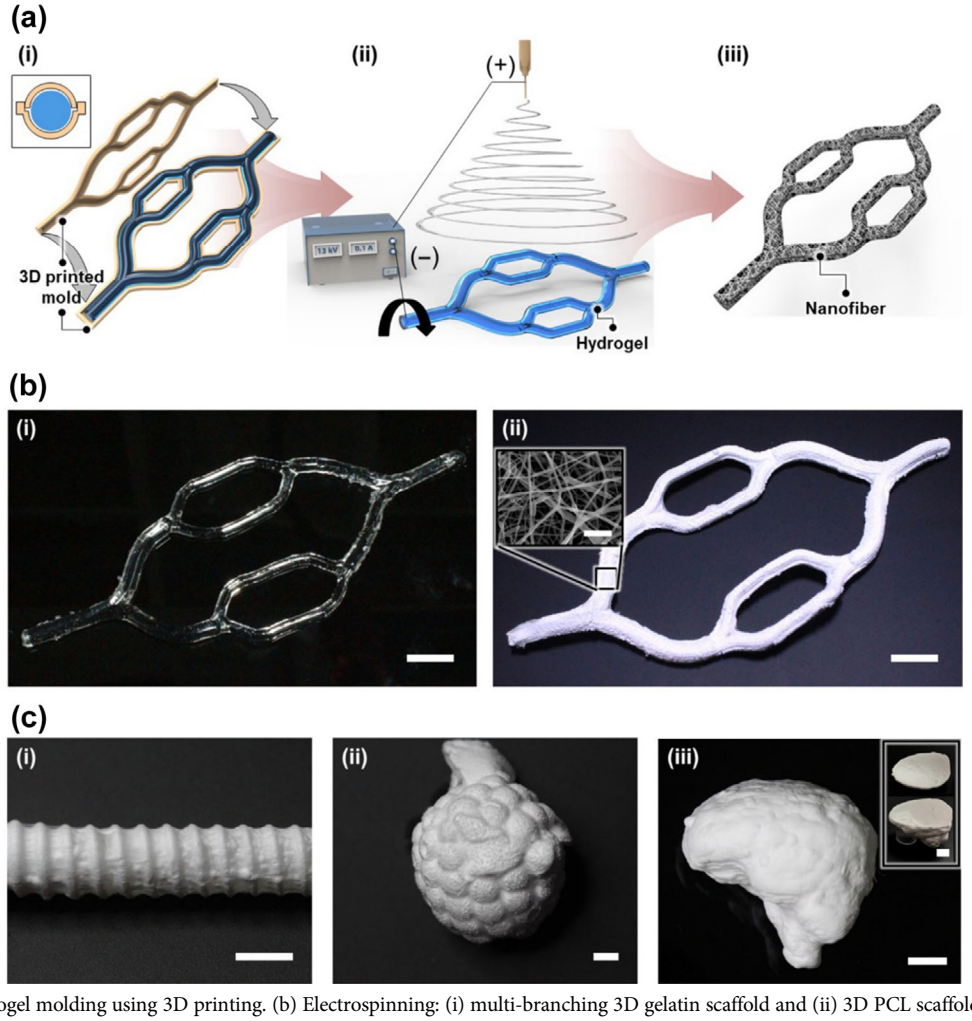

Figure 7 (a) Hydrogel molding using 3D printing. (b) Electrospinning: (i) multi-branching 3D gelatin scaffold and (ii) 3D PCL scaffold. (c) (i) Corrugated tube structure, (ii) small human alveolar structure, and (iii) brain-like shell structure (reproduced with permission from Ref. [125], © American Chemical Society 2020).

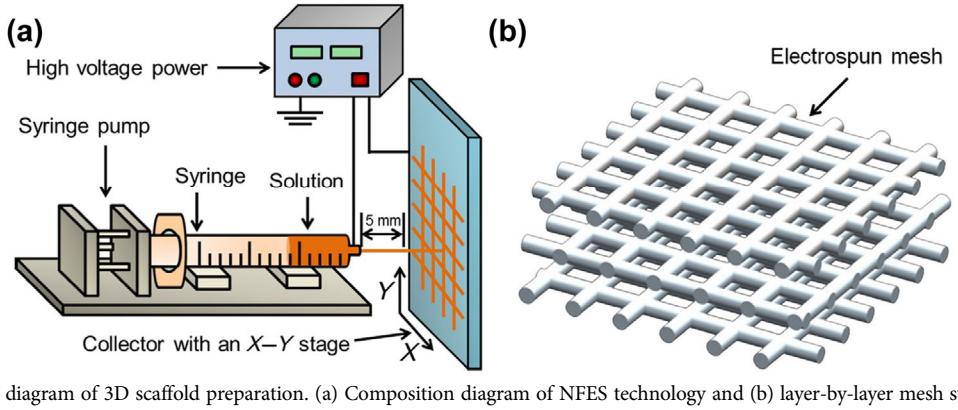

Figure 8 Schematic diagram of 3D scaffold preparation. (a) Composition diagram of NFES technology and (b) layer-by-layer mesh stacking to form a 3D scaffold (reproduced with permission from Ref. [98], © Elsevier B.V. 2017).

performance of hASCs [126]. The scaffold retains the features of the hASC spheroid and can promote angiogenesis.

4.1.2 *Near-field direct write (NFDW) electrospinning*

Owing to the instability of the efflux, electrospinning using conventional solutions produces highly disordered fibers. To enhance the regulation of the deposition location of the electrospun fibers, the distance between the needle and the collector can be reduced to suppress jet instability. However, this reduces the solvent volatilization time and has a significant impact on the fiber mat morphology.

In 2006, Sun et al. proposed a novel electrospinning method called near-field electrospinning (NFES), which was subsequently developed into the NFDW technology [127] and MEW. By lowering the applied voltage and the gap between the spinneret and the receiver, a single fiber with a diameter ranging from a few dozen nanometers to a few hundred microns can be deposited in a direct, continuous, and controllable manner to make characteristic patterns. Notably, this method can be used to fabricate well-supported scaffolds with a large pore size and specific pattern. Consequently, it is widely used in multi-layer tissue engineering scaffold assembly and microelectronics [128].

During melt spinning, owing to the effect of voltage and gravity, and occasionally the air pump pressure, the continuously extruded heated molten polymer forms a filament, whose final diameter depends primarily on the pole size of the nozzle [129]. Through computer control and design, MEW can realize programmable electrospinning, which offers significant control over the fiber deposition location, fiber diameter, and fiber shape. Many synthetic polymers are suitable for MEW, but surface hydrophilic modification is often needed due to hydrophobicity. PCL is the most widely used raw material in NFES, but its high hydrophobicity limits its applications. To improve its hydrophilicity, He et al. mixed a specific ratio of hydroxyapatite (HAp) with PCL and prepared written grids using NFES. The grids were then stacked layer-by-layer to construct a 3D scaffold [98], with the potential to be used for osteogenic repair. The characterization results revealed that this scaffold increases the migration, proliferation rate, and differentiation of bone cells, which is possibly due to its excellent interconnectivity and an average pore size of ~ 167 μm.

Nowadays NFES is no longer limited to melt electrospinning, solutions can also be used in this. Moreover, solution-based and NFES can be used to produce finer fibers than melted polymer-based NFES [130]. Park et al. proposed a precise direct-write 3D nanoprinting process that enables the fabrication of template-free, self-aligned, and self-stacking nanostructures without the need for a collector [131]. The deposition of each layer of the nanofibers can be precisely controlled by simply adding a small amount of salt to the PEO solution. This precise self-stacking phenomenon is related to the dissipated charge in the formed fibers, which is essential for generating inductive forces to accurately guide the nanofiber jets.

4.2 Advantages and considerations of 3D nanofibrous scaffolds

Based on the application, the following factors [132] must be considered while designing electrospun scaffolds: (1) biocompatibility and biotoxicity; (2) mechanical properties and degradation behavior *in vivo*; (3) proper pore size and porosity; and (4) ability to regulate cellular behavior.

In addition to planar structures, electrospun scaffolds can also be developed as curved vascular scaffolds. To improve the biocompatibility of scaffolds, several natural materials are widely used in electrospinning. However, the strength of these natural materials is generally quite low. Therefore, some polymers must be added to the spinning fluid to improve the mechanical properties of the resulting scaffolds. Wu et al. developed a poly(L-lactide-*co*-caprolactone) (P(LLA-CL)), collagen- and chitosan-based tubular scaffold [133] with a symmetric gradient structure using bi-directional electrospinning technology. The scaffold had improved mechanical properties and biocompatibility. Thus, electrospun scaffolds are a promising candidate for vascular engineering.

Compared to 2D wound dressings, 3D scaffolds have better mechanical properties and can support cell adhesion, proliferation, and migration. However, many rigid materials are non-water-soluble, which leads to low biocompatibility. In addition, constructing 3D structures from hydrophilic materials is difficult owing to their low mechanical strength. Gelatin is a biologically friendly material made from animal collagen that has been widely used in medical hydrogels. Gelatin is considered to be highly suitable for biomedical applications as it contains numerous bioactive components, such as arginine-glycine-aspartic acid (RGD) and matrix metalloproteinase (MMP), which enhance cell adhesion and remodeling [134, 135], respectively. However, gelatin is water-soluble and must be cross-linked to maintain its stability in water. Generally, organic reagents such as glutaraldehyde are commonly used as crosslinking agents; however, they can have a negative effect on the security of hydrogels due to their cytotoxicity. Zhao et al. [136] and Gao et al. [85] incorporated methacryloyl groups into gelatin and synthesized optical cross-linkable gelatin methacryloyl (GelMA); subsequently, photo cross-linked hydrogel fibers were prepared by electrospinning. The resultant GelMA electrospun scaffolds have controllable water retention capability and suitable physical and degradation properties. These scaffolds promote wound healing, making them promising candidates for skin regeneration and skin substitutes.

5 Primary applications of electrospun fibers

5.1 Delivery of drugs and other substances

Encapsulation and delivery is an attractive method of trapping drugs and biological components in a polymer material and delivering them to a target, with the aim of preserving the activity of the substances and achieving a controlled release within a set time frame. The main advantages of the electrospinning process over traditional packaging techniques are the absence of heat and their high surface-to-volume ratio, which are important for preserving the structure and achieving a high encapsulation efficiency of the bioactive material during processing and storage [137]. Consequently, substances delivery is one of the most commonly used functions of electrospun fibers.

In addition to direct electrospinning by blending the drug with the spinning solution and embedding the drug in the core layer using coaxial electrospinning, researchers have also attempted to wrap drugs with nanoparticles, followed by electrospinning a mixture of the nanoparticles and the spinning solution to produce drug-carrying fibers. For example, a novel multi-functional dual drug delivery system based on PCL and gelatin was developed [138], wherein indomethacin (IMC) and DOX can be loaded simultaneously. The positions of the drugs in the complex fibers determine their respective release curves. IMC is released rapidly because it is randomly distributed in the fiber matrix, whereas DOX exhibits a persistent long-term release behavior because it is embedded

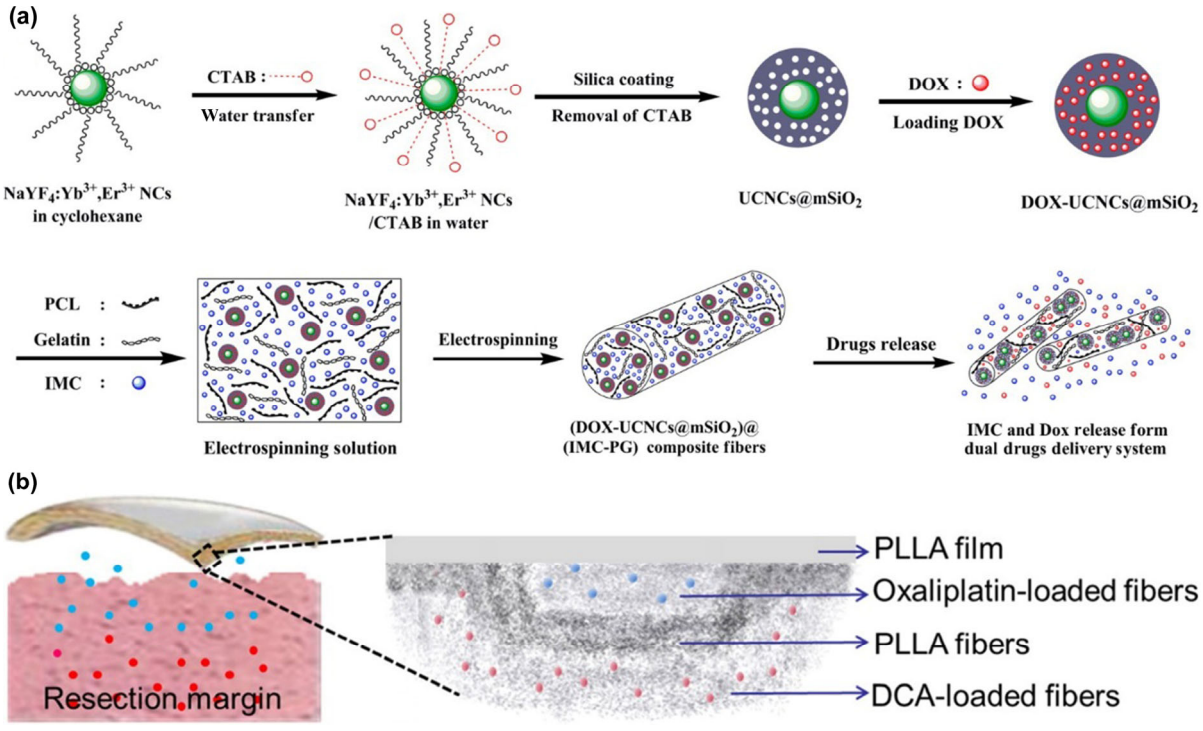

Figure 9 (a) Schematic diagram of the fabrication process of DOX–IMC complex fibers (reproduced with permission from Ref. [138], © American Chemical Society 2013). (b) Multilayered fiber mats loaded with two drugs (DCA and oxaliplatin) (reproduced with permission from Ref. [139], © Elsevier B.V. 2016).

in nanoparticles. Similarly, fibers loaded with two different drugs (dichloroacetate (DCA) and oxaliplatin) in different layers also exhibited a time-programmed double release behavior and had a synergistic effect on tumor cells [139]. The non-toxic DCA selectively accelerates the apoptosis of tumor cells by regulating cell metabolism and oxaliplatin then removes the remaining tumor cells at low concentrations. Besides being applied directly to the affected area, drug-loaded nanofibers can be crushed into micron-sized particles through heat treatment and low-temperature grinding. For instance, PVA fiber granules coated with finasteride can be used as prostatic embolization agents to induce the formation of prostatic lumen and reduce prostatic volume [14].

In addition to drug delivery, electrospinning can also be used to deliver other substances such as viruses [140], microbes [141], and cells [142, 143], as well as bioactive factors such as peptides [144], growth factors [145], and nucleic acids [86, 146, 147]. For example, miRNA-126 mediated by nanofibers can be delivered to vascular endothelial cells for angiogenesis [147], and electrospun fibers with multiple growth factors can release multiple angiogenic growth factors during different stages of chronic wound healing [145]. One interesting study involved the encapsulation of microorganisms in microfibers using electrospinning, wherein the microbes remained intact inside the microfibers [141]. As microbes can be stored at room temperature for a relatively long time, they can be freely transported and activated when required by adding water. In another study [148], an adenovirus was uniformly encapsulated in the core layer of a coaxial electrospun fiber and released through pores created by a pore-forming agent. One of the key findings of this study was that macrophages cultured on virus-coated scaffolds produced lower levels of pro-inflammatory and antiviral cytokines compared to cells that were directly exposed to the adenovirus in a culture medium, which suggests that fibrous encapsulation may reduce the activation of inflammatory cytokines against controlled-release viruses. Overall, the results suggested that coaxial electrospun fibers coated with viruses can promote viral gene transfer in regenerative medicine. Yeast cells can also be encased in the cores of microtubules with non-degradable polymer shells. The electrospun yeast cells exhibited significant phenol bioremediation activity and produced ethanol. Moreover, these cells can be modified to reduce the toxicity of *Escherichia coli* in olive wastewater [143].

5.2 Tissue engineering scaffolds

An ideal scaffold should be able to provide the optimal physiological conditions to guide tissue recombination and degradation within a reasonable time frame, such that the regenerated tissue can be integrated with the host. Accordingly, the physical properties of the scaffold must be designed based on the surrounding environment of the implant site.

Skin engineering: Electrospun nanofibers have high porosity and excellent hygroscopicity and air permeability. In addition, owing to their excellent drug-loading properties, they have a certain amount of antibacterial and anti-inflammatory activity [152]. These advantages make electrospun nanofibers an excellent choice for preparing wound dressings. Generally, healthy skin includes the epidermis, dermis, and subcutaneous tissue from outside to inside, which acts as a stable barrier between the internal regions of the body and the outside environment and offers protection against external damage. Keratinocytes and fibroblasts are present in the epidermis. Both of them bind tightly to fibers such as collagen, fibrinogen, and elastin, and veins and lymphatics run through them to provide the required nutrients and immune activity. Owing to the dense structure and functional characteristics of nanofiber wound dressings, they not only serve as antibacterial devices that promote wound repair or achieve rapid hemostasis of the wound, but also as a skin barrier to prevent internal tissues from mechanical impact and microbial infections. The addition of Cu_2S to the fibers and the application of near-infrared (NIR) radiation create a photothermal effect that can kill skin cancer cells [149] (Fig. 10(a)). Recently,

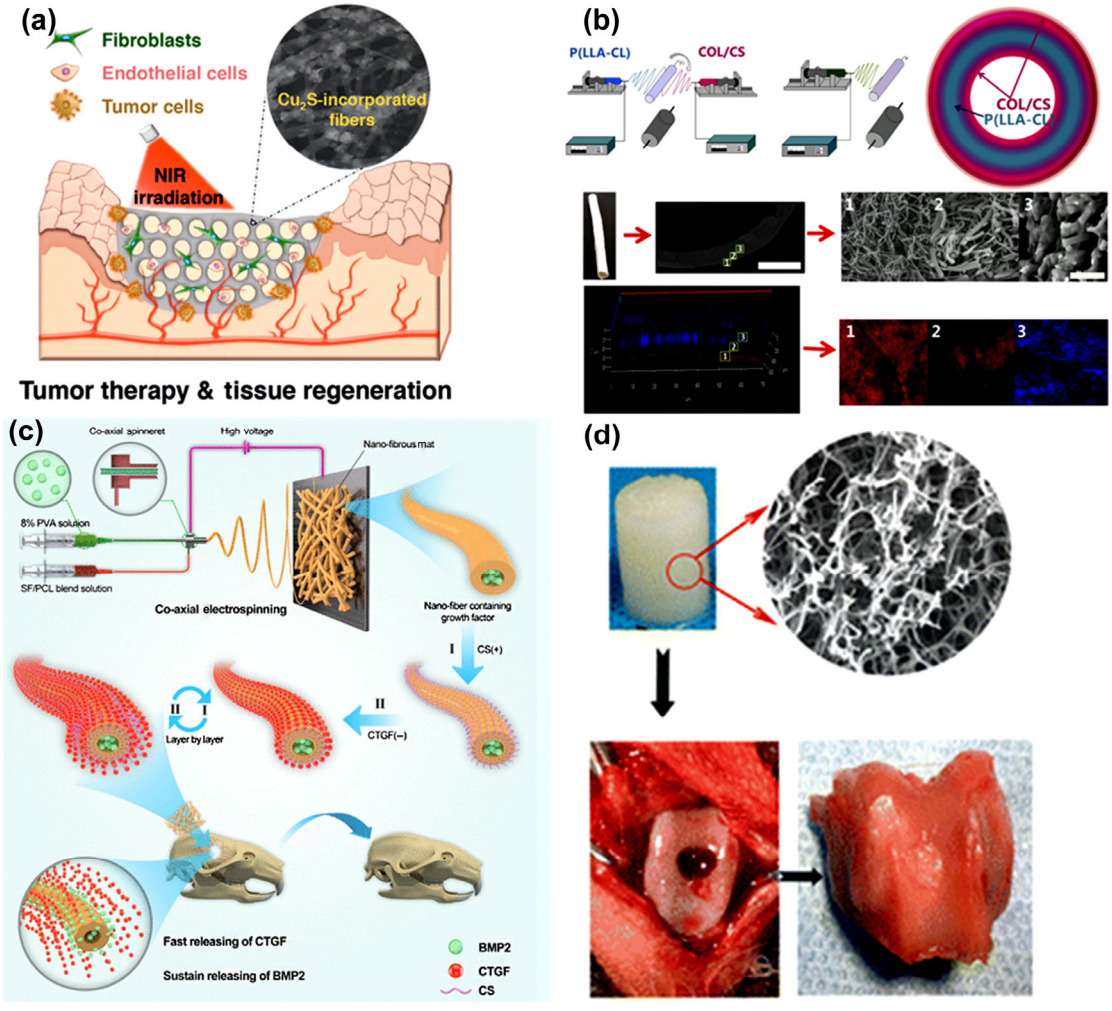

Figure 10 (a) Wound dressing for diabetes foot ulcer healing (reproduced with permission from Ref. [149], © American Chemical Society 2017). (b) Bilayer vascular scaffold with gradient structure fabricated using bi-directional electrospinning (reproduced with permission from Ref. [133], © Elsevier B.V. 2015). (c) Bone regeneration scaffold consisting of layers of assembled core–shell nanofibers (reproduced with permission from Ref. [150], © American Chemical Society 2019). (d) Gelatin/PLA 3D scaffold for rabbit cartilage repair (reproduced with permission from Ref. [151], © American Chemical Society 2016).

portable electrospinning machines have been widely used to realize *in situ* deposition of fibers for wound coverage and rapid hemostasis. This technology allows fibrous membranes to form directly on the wound bed in a few minutes [153].

Another bioderived scaffold is a dermal replacement, which may consist of autologous derived cells and can act as a dermal layer to aid wound healing [154]. The structure of electrospun fibers can be manipulated to mimic human epithelial tissue. Together with a variety of strategies for integrating antimicrobial substances, these scaffolds can also prevent infection. Studies have shown that scaffolds with corresponding dermal seed cells have better wound healing performance than those without cells [154, 155]. Revero et al. transplanted Wharton's jelly mesenchymal stem cells (WJ-MSCs) into a silk fibroin protein scaffold; the results showed that the scaffold could promote the generation of vascular granulation tissue, accelerate re-epithelialization, and reduce the formation of fibrotic scar tissue [156]. Thus, the preparation of tissue engineering scaffolds that can support seed cells is another highlight of electrospinning technology.

Vascular engineering: Vascular scaffolds play an important role in the formation of functional blood vessels that can not only withstand physiological hemodynamic forces, but also maintain structural integrity until new blood vessels are formed [157]. Blood vessels have a stratified structure, with an inner layer composed of endothelial cells attached to a membrane and an outer layer composed of vascular smooth muscle cells. Therefore, electrospinning is widely used to produce double-layer scaffold structures to support the growth of these two types of cells [158, 159]. For example, a bi-layered vascular scaffold (Fig. 10(b)) with a symmetric gradient structure fabricated through bi-directional electrospinning technology has significant potential as a vascular graft [133].

Bone regeneration: Bone tissue engineering (BTE) focuses on bone repair. When a bone defect exceeds the self-healing ability of the body, a bone graft can be implanted to help regenerate the bone. Electrospun scaffolds can mimic the fibrillary structure of the bone ECM. Therefore, bone grafts that are suitable for BTE can be obtained by processing bioactive glass and calcium phosphate using electrospinning [160]. In particular, the silica of bioglass materials has a positive effect on type I collagen synthesis and matrix mineralization and osteoblast differentiation [161], and hydroxyapatite is an important bone component. Growth factors also play an important role in bone regeneration. Cheng et al. used layers of assembled core–shell nanofibers to encapsulate bone morphogenetic protein 2 (BMP-2) and connective tissue growth factor (CTGF) to achieve time-coordinated release (Fig. 10(c)). This scaffold provides significant improvements in angiogenesis and bone tissue recovery [150] as the

continuous release of BMP-2 enhances bone formation, and the instantaneous release of CTGF promotes angiogenesis during bone healing.

Cartilage repair: Cartilage is composed of a collagen fiber network and hydrated proteoglycan matrix, which gives tissues complex mechanical properties such as viscoelasticity and stress relaxation [162], and is vital for the carrying capacity of human organs. Chen et al. developed a 3D scaffold consisting of electrospun gelatin/PLA nanofibers [151]. The 3D scaffold structure, which was fabricated by simply electrospinning gelatin and PLA followed by freeze-drying and heat treatment, showed a strong ability to repair cartilage defects in rabbits (Fig. 10(d)). Owing to the thickness and hardness of cartilage, the melt direct writing technique is a popular method of constructing artificial cartilage scaffolds [163, 164], as it can produce scaffolds with a certain thickness and can guide the orientation of tissue and fibrous matrix. Chen et al. used this technique to create a scaffold that mimics the tissue in the region of the articular cartilage. Compared to conventional electrospun scaffolds, the expression of cartilage markers in this scaffold was significantly higher [164].

5.3 Other applications

In addition to tissue-engineering applications, the remarkable properties of electrospun fibers make them useful for several other applications. For example, electrospun fibers have excellent piezoelectric properties, and their wide dynamic pressure sensing ability can realize the accurate measurement of the fine static pressure on human skin; therefore, they are suitable as bioelectronic skin sensors [165]. Besides, electrospinning also has significant potential for application in minimally invasive operations (MIOs) for hemostasis. During a case of MIOs in pigs, Zhang et al. embedded long needles in a laparoscopic tube to deposit electrospun nanofibers *in situ* on the wound surface [166] instead of pressing electrospun mats prepared *in vitro* on the surface of living organs. The precise deposition of nanofibers can be achieved by introducing an electric field convergence structure at the tip of the needle. Compared to traditional hemostasis methods such as sutures and cotton pressure, this method provides a shorter hemostasis time, less postoperative inflammatory reaction, and faster recovery. Furthermore, nanocarbons (carbon nanotubes, graphene, fullerenes, and their derivatives) can be incorporated into electrospun polymer fibers to improve their functionality [167]. Electrospun polymer nanocomposites can be used to improve mechanical, electrical, and thermal properties, and implant biological functionality into scaffolds in biomedical engineering and sensors.

6 Conclusion and prospects

In this review, the common 2D morphological and 3D topological structures of electrospun nanofibers fabricated for biomedical applications were listed, and their corresponding characteristics and biomedical applications were discussed in detail. Various fibrous structures have been designed to match the composition of different tissues in the body, and their application characteristics listed in this review are summarized in Table 4.

Electrospinning technology has developed significantly over the past few decades; however, there are still several areas that require improvements. These include methods to obtain a stable yield of nanofibers, control the fiber diameter, fabricate fibers with a specific pore size and porosity, precisely control deposited nanofibers in specific locations and directions, and achieve mass production [92]. Significant efforts have been devoted to improving the construction and application of biomimetic scaffolds in recent years. Nevertheless, these scaffolds are still inferior to the natural body and substantial improvements are required to better mimic the physiological environment of tissue cells.

The main limitations of electrospinning are its low yield and long preparation time, which limits its large-scale commercial development. Therefore, techniques to improve the yield and efficiency of electrospinning are an important area of research. Accordingly, needle-free electrospinning, multi-needle electrospinning, and pulse gas-assisted electrospinning technology have been developed to accelerate the spinning speed and achieve batch production. Multi-needle electrospinning uses a multi-needle to increase the liquid output of the spinning liquid. To obtain uniform fibers with high productivity, auxiliary plate electrodes are connected to multi-needle systems to obtain a more uniform electric field [172]. The larger the number of needles, the higher the average electric field intensity and the smaller the average fiber diameter [173]. Needle-free electrospinning is based on the process of fiber self-formation induced by electrospinning on open surfaces [174]. Electrospinning occurs directly on the surface of the solution and produces multiple Taylor cones, with varied fiber geometry. Although these technologies have effectively improved the fiber yield of electrospinning, significant improvements are required to achieve industrial mass production.

Another medical disadvantage of electrospinning is that the instruments are bulky and must be connected to a high-voltage power supply, which limits its clinical applications. In recent years, portable handheld electrospinning equipment has been developed for direct applications in clinics. However, these developments primarily focus on the technical design of

Table 4 Nanofiber structures and their corresponding biomedical applications

Structure of nanofibers	Corresponding applications
Homogeneous nanofibers	The most basic structure, suitable for a variety of applications [12, 13]
Coaxial nanofibers	Controlled drug release, biological sensing [16, 17, 29]
Nanofiber yarns and bundles	Surgical sutures and woven wound dressing [57, 61]
Bead-on-string nanofibers	Drug carrying and delivery [41, 45]
Helical nanofibers	Collagen mats, potential to mimic DNA structure [168]
Randomly-oriented fibers	Wound dressings [169]
Aligned nanofibers	Tissues with oriented fibrous structures such as nerve ducts, tendons, and ligaments [170]
Gradient nanofibers	Parts of the body formed by multiple layers of tissue with different characteristics, such as skin or cartilage [171]
Nanofibers with large pores	Promote cell infiltration and growth [98]
3D structures	Promote cell infiltration, repair large defects such as in bones; biological substitutes, such as blood vessels, ligaments, and epidermis [125, 151]

the equipment, and obstacles, such as the selection of polymers, solvents, and additives, still exist, which limits its application. To improve the *in situ* deposition curative effect, toxic solvents should be avoided and the fibers should be derived from an appropriate polymer based on the configuration of the wound bed [153].

In general, electrospinning can produce several fibers that mimic the various morphologies and structures of human tissue, making it a popular method of constructing tissue-engineered scaffolds. However, obstacles such as low output and large machine size still limit its range of application. Electrospinning is extensively studied by numerous researchers and continues to develop rapidly, making it a very promising technology.

Acknowledgements

We sincerely acknowledge the funding from Medical Scientific Research Foundation of Guangdong Province (No. A2021093), Science and Technology Planning Project of Shenzhen Municipality (No. YJ20180306174831458), Shenzhen Basic Research Project (No. JCYJ20190807155801657), National Science and Technology Major Project of the Ministry of Science and Technology of China (No. 2018ZX10301402), Key International (Regional) Joint Research Program of China (No. 5181001045), Guangdong Innovative and Entrepreneurial Research Team Program (No. 2016ZT06S029), and the National Natural Science Foundation of China (No. 51973243), China Postdoctoral Science Foundation (No. 2019M663246), the Fundamental Research Funds for the Central Universities (Nos. 191gzd35 and 20ykpy15), and Guangdong Basic and Applied Basic Research Foundation (No. 2019A1515110686).

References

[1] Keirouz, A.; Chung, M.; Kwon, J.; Fortunato, G.; Radacsi, N. 2D and 3D electrospinning technologies for the fabrication of nanofibrous scaffolds for skin tissue engineering: A review. *Wiley Interdiscip Rev. Nanomed. Nanobiotechnol.* **2020**, *12*, e1626.

[2] Teo, W. E.; Ramakrishna, S. A review on electrospinning design and nanofibre assemblies. *Nanotechnology* **2006**, *17*, R89-R106.

[3] Li, D.; Xia, Y. N. Electrospinning of nanofibers: Reinventing the wheel? *Adv. Mater.* **2004**, *16*, 1151–1170.

[4] Zhang, C. L.; Yu, S. H. Spraying functional fibres by electrospinning. *Mater. Horiz.* **2016**, *3*, 266–269.

[5] Liu, G. T.; Bao, Z. T.; Wu, J. Injectable baicalin/F127 hydrogel with antioxidant activity for enhanced wound healing. *Chin. Chem. Lett.* **2020**, *31*, 1817–1821.

[6] Gao, Y. F.; Li, Z.; Huang, J.; Zhao, M.; Wu, J. *In situ* formation of injectable hydrogels for chronic wound healing. *J. Mater. Chem. B* **2020**, *8*, 8768–8780.

[7] Xue, J. J.; Pisignano, D.; Xia, Y. N. Maneuvering the migration and differentiation of stem cells with electrospun nanofibers. *Adv. Sci.* **2020**, *7*, 2000735.

[8] Karimi, F.; O'Connor, A. J.; Qiao, G. G.; Heath, D. E. Integrin clustering matters: A review of biomaterials functionalized with multivalent integrin-binding ligands to improve cell adhesion, migration, differentiation, angiogenesis, and biomedical device integration. *Adv. Healthc. Mater.* **2018**, *7*, 1701324.

[9] Ding, J. X.; Zhang, J.; Li, J. N.; Li, D.; Xiao, C. S.; Xiao, H. H.; Yang, H. H.; Zhuang, X. L.; Chen, X. S. Electrospun polymer biomaterials. *Prog. Polym. Sci.* **2019**, *90*, 1–34.

[10] Chen, S. X.; Li, R. Q.; Li, X. R.; Xie, J. W. Electrospinning: An enabling nanotechnology platform for drug delivery and regenerative medicine. *Adv. Drug Deliv. Rev.* **2018**, *132*, 188–213.

[11] Arasu, V.; Hwang, S.; Zhang, B.; Byun, D.; Park, S. H. 1D fibers and 2D patterns made of quantum dot-embedded DNA via electrospinning and electrohydrodynamic jet printing. *Adv. Mater. Technol.* **2019**, *4*, 1800280.

[12] Greiner, A.; Wendorff, J. H. Electrospinning: A fascinating method for the preparation of ultrathin fibers. *Angew. Chem., Int. Ed.* **2007**, *46*, 5670–5703.

[13] Chen, Z. G.; Mo, X. M.; Qing, F. L. Electrospinning of collagen–chitosan complex. *Mater. Lett.* **2007**, *61*, 3490–3494.

[14] Li, X. H.; Li, B. S.; Ullah, M. W.; Panday, R.; Cao, J. M.; Li, Q. B.; Zhang, Y. P.; Wang, L.; Yang, G. Water-stable and finasteride-loaded polyvinyl alcohol nanofibrous particles with sustained drug release for improved prostatic artery embolization—*in vitro* and *in vivo* evaluation. *Mater. Sci. Eng.: C* **2020**, *115*, 111107.

[15] Hou, L. L.; Wang, N.; Wu, J.; Cui, Z. M.; Jiang, L.; Zhao, Y. Bioinspired superwettability electrospun micro/nanofibers and their applications. *Adv. Funct. Mater.* **2018**, *28*, 1801114.

[16] Yarin, A. L. Coaxial electrospinning and emulsion electrospinning of core–shell fibers. *Polym. Adv. Technol.* **2011**, *22*, 310–317.

[17] He, P.; Zhong, Q.; Ge, Y.; Guo, Z. Z.; Tian, J. H.; Zhou, Y. H.; Ding, S.; Li, H.; Zhou, C. R. Dual drug loaded coaxial electrospun PLGA/PVP fiber for guided tissue regeneration under control of infection. *Mater. Sci. Eng.: C* **2018**, *90*, 549–556.

[18] Zhao, Y.; Cao, X. Y.; Jiang, L. Bio-mimic multichannel microtubes by a facile method. *J. Am. Chem. Soc.* **2007**, *129*, 764–765.

[19] Ji, W.; Yang, F.; van den Beucken, J. J. J. P.; Bian, Z.; Fan, M. W.; Chen, Z.; Jansen, J. A. Fibrous scaffolds loaded with protein prepared by blend or coaxial electrospinning. *Acta Biomater.* **2010**, *6*, 4199–4207.

[20] Li, L. L.; Peng, S. J.; Cheah, Y. L.; Wang, J.; Teh, P.; Ko, Y.; Wong, C.; Srinivasan, M. Electrospun eggroll-like $CaSnO_3$ nanotubes with high lithium storage performance. *Nanoscale* **2013**, *5*, 134–138.

[21] Sun, Z.; Zussman, E.; Yarin, A. L.; Wendorff, J. H.; Greiner, A. Compound core–shell polymer nanofibers by co-electrospinning. *Adv. Mater.* **2003**, *15*, 1929–1932.

[22] Zussman, E.; Yarin, A. L.; Bazilevsky, A. V.; Avrahami, R.; Feldman, M. Electrospun polyaniline/poly(methyl methacrylate)-derived turbostratic carbon micro-/nanotubes. *Adv. Mater.* **2006**, *18*, 348–353.

[23] Moreno, I.; González-González, V.; Romero-García, J. Control release of lactate dehydrogenase encapsulated in poly (vinyl alcohol) nanofibers via electrospinning. *Eur. Polym. J.* **2011**, *47*, 1264–1272.

[24] Zhang, C.; Feng, F. Q.; Zhang, H. Emulsion electrospinning: Fundamentals, food applications and prospects. *Trends Food Sci. Technol.* **2018**, *80*, 175–186.

[25] Li, X. L.; Xu, F. N.; He, Y.; Li, Y.; Hou, J. W.; Yang, G.; Zhou, S. B. A hierarchical structured ultrafine fiber device for preventing postoperative recurrence and metastasis of breast cancer. *Adv. Funct. Mater.* **2020**, *30*, 2004851.

[26] Rathore, P.; Schiffman, J. D. Beyond the single-nozzle: Coaxial electrospinning enables innovative nanofiber chemistries, geometries, and applications. *ACS Appl. Mater. Interfaces* **2021**, *13*, 48–66.

[27] Pakravan, M.; Heuzey, M. C.; Ajji, A. Core–shell structured PEO-chitosan nanofibers by coaxial electrospinning. *Biomacromolecules* **2012**, *13*, 412–421.

[28] Liu, X. K.; Yang, Y. Y.; Yu, D. G.; Zhu, M. J.; Zhao, M.; Williams, G. R. Tunable zero-order drug delivery systems created by modified triaxial electrospinning. *Chem. Eng. J.* **2019**, *356*, 886–894.

[29] Li, L. L.; Peng, S. J.; Lee, J. K. Y.; Ji, D. X.; Srinivasan, M.; Ramakrishna, S. Electrospun hollow nanofibers for advanced secondary batteries. *Nano Energy* **2017**, *39*, 111–139.

[30] Yoon, J.; Yang, H. S.; Lee, B. S.; Yu, W. R. Recent progress in coaxial electrospinning: New parameters, various structures, and wide applications. *Adv. Mater.* **2018**, *30*, 1704765.

[31] Ou, K. L.; Chen, C. S.; Lin, L. H.; Lu, J. C.; Shu, Y. C.; Tseng, W. C.; Yang, J. C.; Lee, S. Y.; Chen, C. C. Membranes of epitaxial-like packed, super aligned electrospun micron hollow poly(l-lactic acid) (PLLA) fibers. *Eur. Polym. J.* **2011**, *47*, 882–892.

[32] Halaui, R.; Zussman, E.; Khalfin, R.; Semiat, R.; Cohen, Y. Polymeric microtubes for water filtration by co-xial electrospinning technique. *Polym. Adv. Technol.* **2017**, *28*, 570–582.

[33] Yang, H. S.; Lee, B. S.; You, B. C.; Sohn, H. J.; Yu, W. R. Fabrication of carbon nanofibers with Si nanoparticle-stuffed cylindrical multi-channels via coaxial electrospinning and their anodic performance. *RSC Adv.* **2014**, *4*, 47389–47395.

[34] Jeong, Y. J.; Koo, W. T.; Jang, J. S.; Kim, D. H.; Kim, M. H.; Kim, I. D. Nanoscale PtO_2 catalysts-loaded SnO_2 multichannel nanofibers toward highly sensitive acetone sensor. *ACS Appl. Mater. Interfaces* **2018**, *10*, 2016–2025.
[35] Fong, H.; Chun, I.; Reneker, D. H. Beaded nanofibers formed during electrospinning. *Polymer* **1999**, *40*, 4585–4592.
[36] Shenoy, S. L.; Bates, W. D.; Frisch, H. L.; Wnek, G. E. Role of chain entanglements on fiber formation during electrospinning of polymer solutions: Good solvent, non-specific polymer–polymer interaction limit. *Polymer* **2005**, *46*, 3372–3384.
[37] Lin, T.; Wang, H. X.; Wang, H. M.; Wang, X. G. The charge effect of cationic surfactants on the elimination of fibre beads in the electrospinning of polystyrene. *Nanotechnology* **2004**, *15*, 1375–1381.
[38] Zuo, W. W.; Zhu, M. F.; Yang, W.; Yu, H.; Chen, Y. M.; Zhang, Y. Experimental study on relationship between jet instability and formation of beaded fibers during electrospinning. *Polym. Eng. Sci.* **2005**, *45*, 704–709.
[39] Liu, Y.; He, J. H.; Yu, J. Y.; Zeng, H. M. Controlling numbers and sizes of beads in electrospun nanofibers. *Polym. Int.* **2008**, *57*, 632–636.
[40] Tian, X. L.; Bai, H.; Zheng, Y. M.; Jiang, L. Bio-inspired heterostructured bead-on-string fibers that respond to environmental wetting. *Adv. Funct. Mater.* **2011**, *21*, 1398–1402.
[41] Somvipart, S.; Kanokpanont, S.; Rangkupan, R.; Ratanavaraporn, J.; Damrongsakkul, S. Development of electrospun beaded fibers from Thai silk fibroin and gelatin for controlled release application. *Int. J. Biol. Macromol.* **2013**, *55*, 176–184.
[42] Li, T. X.; Ding, X.; Tian, L. L.; Hu, J. Y.; Yang, X. D.; Ramakrishna, S. The control of beads diameter of bead-on-string electrospun nanofibers and the corresponding release behaviors of embedded drugs. *Mater. Sci. Eng.: C* **2017**, *74*, 471–477.
[43] Greenfeld, I.; Rodricks, C. W.; Sui, X. M.; Wagner, H. D. Beaded fiber composites—Stiffness and strength modeling. *J. Mech. Phys. Solids* **2019**, *125*, 384–400.
[44] Li, T. X.; Wang, L.; Huang, Y. F.; Xin, B. J.; Liu, S. BSA loaded bead-on-string nanofiber scaffold with core-shell structure applied in tissue engineering. *J. Biomater. Sci., Polym. Ed.* **2020**, *31*, 1223–1236.
[45] Xi, H. J.; Zhao, H. J. Silk fibroin coaxial bead-on-string fiber materials and their drug release behaviors in different pH. *J. Mater. Sci.* **2019**, *54*, 4246–4258.
[46] Rasouli, M.; Pirsalami, S.; Zebarjad, S. M. Study on the formation and structural evolution of bead-on-string in electrospun polysulfone mats. *Polym. Int.* **2020**, *69*, 822–832.
[47] Bu, N. B.; Huang, Y. A.; Deng, H. X.; Yin, Z. P. Tunable bead-on-string microstructures fabricated by mechano-electrospinning. *J. Phys. D: Appl. Phys.* **2012**, *45*, 405301.
[48] Wang, Z.; Zhao, C. C.; Pan, Z. J. Porous bead-on-string poly(lactic acid) fibrous membranes for air filtration. *J. Colloid Interface Sci.* **2015**, *441*, 121–129.
[49] Gupta, P.; Elkins, C.; Long, T. E.; Wilkes, G. L. Electrospinning of linear homopolymers of poly(methyl methacrylate): Exploring relationships between fiber formation, viscosity, molecular weight and concentration in a good solvent. *Polymer* **2005**, *46*, 4799–4810.
[50] Abutaleb, A.; Lolla, D.; Aljuhani, A.; Shin, H. U.; Rajala, J. W.; Chase, G. G. Effects of surfactants on the morphology and properties of electrospun polyetherimide fibers. *Fibers* **2017**, *5*, 33.
[51] Yu, J.; Qiu, Y. J.; Zha, X. X.; Yu, M.; Yu, J. L.; Rafique, J.; Yin, J. Production of aligned helical polymer nanofibers by electrospinning. *Eur. Polym. J.* **2008**, *44*, 2838–2844.
[52] Kessick, R.; Tepper, G. Microscale polymeric helical structures produced by electrospinning. *Appl. Phys. Lett.* **2004**, *84*, 4807–4809.
[53] Dabirian, F.; Hosseini Ravandi, S. A.; Hashemi Sanatgar, R.; Hinestroza, J. P. Manufacturing of twisted continuous PAN nanofiber yarn by electrospinning process. *Fibers Polym.* **2011**, *12*, 610–615.
[54] Silva, P. E. S.; Vistulo de Abreu, F.; Godinho, M. H. Shaping helical electrospun filaments: A review. *Soft Matter* **2017**, *13*, 6678–6688.
[55] Fennessey, S. F.; Farris, R. J. Fabrication of aligned and molecularly oriented electrospun polyacrylonitrile nanofibers and the mechanical behavior of their twisted yarns. *Polymer* **2004**, *45*, 4217–4225.
[56] Affdl, J. C. H.; Kardos, J. L. The Halpin–Tsai equations: A review. *Polym. Eng. Sci.* **1976**, *16*, 344–352.
[57] Ko, F.; Gogotsi, Y.; Ali, A.; Naguib, N.; Ye, H.; Yang, G. L.; Li, C.; Willis, P. Electrospinning of continuous carbon nanotube-filled nanofiber yarns. *Adv. Mater.* **2003**, *15*, 1161–1165.
[58] Liu, C. K.; Sun, R. J.; Lai, K.; Sun, C. Q.; Wang, Y. W. Preparation of short submicron-fiber yarn by an annular collector through electrospinning. *Mater. Lett.* **2008**, *62*, 4467–4469.
[59] Nakashima, R.; Watanabe, K.; Lee, Y.; Kim, B. S.; Kim, I. S. Mechanical properties of poly(vinylidene fluoride) nanofiber filaments prepared by electrospinning and twisting. *Adv. Polym. Technol.* **2013**, *32*, E44–E52.
[60] O'Connor, R. A.; McGuinness, G. B. Electrospun nanofibre bundles and yarns for tissue engineering applications: A review. *Proc. Inst. Mech. Eng., Part H: J. Eng. Med.* **2016**, *230*, 987–998.
[61] Wu, J. L.; Liu, S.; He, L. P.; Wang, H. S.; He, C. L.; Fan, C. Y.; Mo, X. M. Electrospun nanoyarn scaffold and its application in tissue engineering. *Mater. Lett.* **2012**, *89*, 146–149.
[62] Wu, J. L.; Huang, C.; Liu, W.; Yin, A. L.; Chen, W. M.; He, C. L.; Wang, H. S.; Liu, S.; Fan, C. Y.; Bowlin, G. L. et al. Cell infiltration and vascularization in porous nanoyarn scaffolds prepared by dynamic liquid electrospinning. *J. Biomed. Nanotechnol.* **2014**, *10*, 603–614.
[63] Maleki, H.; Gharehaghaji, A. A.; Toliyat, T.; Dijkstra, P. J. Drug release behavior of electrospun twisted yarns as implantable medical devices. *Biofabrication* **2016**, *8*, 035019.
[64] Burger, C.; Hsiao, B. S.; Chu, B. J. M. Nanofibrous materials and their applications. *Ann. Rev. Mater. Res.* **2006**, *36*, 333–368.
[65] Mushi, N. E.; Kochumalayil, J.; Cervin, N. T.; Zhou, Q.; Berglund, L. A. Nanostructurally controlled hydrogel based on small-diameter native chitin nanofibers: Preparation, structure, and properties. *ChemSusChem* **2016**, *9*, 989–995.
[66] Wang, M. X.; Huang, Z. H.; Kang, F. Y.; Liang, K. M. Porous carbon nanofibers with narrow pore size distribution from electrospun phenolic resins. *Mater. Lett.* **2011**, *65*, 1875–1877.
[67] Han, J. P.; Xiong, L. K.; Jiang, X. Y.; Yuan, X. Y.; Zhao, Y.; Yang, D. Y. Bio-functional electrospun nanomaterials: From topology design to biological applications. *Prog. Polym. Sci.* **2019**, *91*, 1–28.
[68] Naveen, N.; Kumar, R.; Balaji, S.; Uma, T. S.; Natrajan, T. S.; Sehgal, P. K. Synthesis of nonwoven nanofibers by electrospinning – a promising biomaterial for tissue engineering and drug delivery. *Adv. Eng. Mater.* **2010**, *12*, B380–B387.
[69] Li, D.; Wang, Y.; Xia, Y. Electrospinning nanofibers as uniaxially aligned arrays and layer-by-layer stacked films. *Adv. Mater.* **2004**, *16*, 361–366.
[70] Liu, Y. Q.; Zhang, X. P.; Xia, Y. N.; Yang, H. Magnetic-field-assisted electrospinning of aligned straight and wavy polymeric nanofibers. *Adv. Mater.* **2010**, *22*, 2454–2457.
[71] Yuan, H. H.; Zhao, S. F.; Tu, H. B.; Li, B. Y.; Li, Q.; Feng, B.; Peng, H. J.; Zhang, Y. Z. Stable jet electrospinning for easy fabrication of aligned ultrafine fibers. *J. Mater. Chem.* **2012**, *22*, 19634–19638.
[72] Yi, B. C.; Zhang, H. L.; Yu, Z. P.; Yuan, H. H.; Wang, X. L.; Zhang, Y. Z. Fabrication of high performance silk fibroin fibers via stable jet electrospinning for potential use in anisotropic tissue regeneration. *J. Mater. Chem. B* **2018**, *6*, 3934–3945.
[73] Yi, B. C.; Shen, Y. B.; Tang, H.; Wang, X. L.; Li, B.; Zhang, Y. Z. Stiffness of aligned fibers regulates the phenotypic expression of vascular smooth muscle cells. *ACS Appl. Mater. Interfaces* **2019**, *11*, 6867–6880.
[74] Wang, L.; Chang, M. W.; Ahmad, Z.; Zheng, H. X.; Li, J. S. Mass and controlled fabrication of aligned PVP fibers for matrix type antibiotic drug delivery systems. *Chem. Eng. J.* **2017**, *307*, 661–669.
[75] Zhang, J. Y.; Chen, H. L.; Zhao, M.; Liu, G. T.; Wu, J. 2D nanomaterials for tissue engineering application. *Nano Res.* **2020**, *13*, 2019–2034.
[76] Jun, I.; Chung, Y. W.; Heo, Y. H.; Han, H. S.; Park, J.; Jeong, H.; Lee, H.; Lee, Y. B.; Kim, Y. C.; Seok, H. K. et al. Creating hierarchical topographies on fibrous platforms using femtosecond laser ablation for directing myoblasts behavior. *ACS Appl. Mater. Interfaces* **2016**, *8*, 3407–3417.
[77] Ren, X. Z.; Li, J. X.; Li, J. Y.; Jiang, Y. Q.; Li, L.; Yao, Q. Q.; Ke, Q. F.; Xu, H. Aligned porous fibrous membrane with a biomimetic surface to accelerate cartilage regeneration. *Chem. Eng. J.* **2019**, *370*, 1027–1038.

[78] Brennan, D. A.; Conte, A. A.; Kanski, G.; Turkula, S.; Hu, X.; Kleiner, M. T.; Beachley, V. Mechanical considerations for electrospun nanofibers in tendon and ligament repair. *Adv. Healthc. Mater.* **2018**, *7*, 1701277.

[79] Deepthi, S.; Nivedhitha Sundaram, M.; Deepti Kadavan, J.; Jayakumar, R. Layered chitosan-collagen hydrogel/aligned PLLA nanofiber construct for flexor tendon regeneration. *Carbohydr. Polym.* **2016**, *153*, 492–500.

[80] Zhu, L.; Jia, S. J.; Liu, T. J.; Yan, L.; Huang, D. G.; Wang, Z. Y.; Chen, S.; Zhang, Z. P.; Zeng, W.; Zhang, Y. et al. Aligned PCL fiber conduits immobilized with nerve growth factor gradients enhance and direct sciatic nerve regeneration. *Adv. Funct. Mater.* **2020**, *30*, 2002610.

[81] Zou, Y. W.; Qin, J. B.; Huang, Z. B.; Yin, G. F.; Pu, X. M.; He, D. Fabrication of aligned conducting PPy-PLLA fiber films and their electrically controlled guidance and orientation for neurites. *ACS Appl. Mater. Interfaces* **2016**, *8*, 12576–12582.

[82] Yeo, M.; Kim, G. H. Anisotropically aligned cell-laden nanofibrous bundle fabricated via cell electrospinning to regenerate skeletal muscle tissue. *Small* **2018**, *14*, 1803491.

[83] Li, X. R.; Li, M. Y.; Sun, J.; Zhuang, Y.; Shi, J. J.; Guan, D. W.; Chen, Y. Y.; Dai, J. W. Radially aligned electrospun fibers with continuous gradient of SDF1α for the guidance of neural stem cells. *Small* **2016**, *12*, 5009–5018.

[84] Wu, T.; Xue, J. J.; Xia, Y. N. Engraving the surface of electrospun microfibers with nanoscale grooves promotes the outgrowth of neurites and the migration of schwann cells. *Angew. Chem., Int. Ed.* **2020**, *59*, 15626–15632.

[85] Gao, X. Z.; Han, S. Y.; Zhang, R. H.; Liu, G. T.; Wu, J. Progress in electrospun composite nanofibers: Composition, performance and applications for tissue engineering. *J. Mater. Chem. B* **2019**, *7*, 7075–7089.

[86] Nguyen, L. H.; Gao, M. Y.; Lin, J. Q.; Wu, W. T.; Wang, J.; Chew, S. Y. Three-dimensional aligned nanofibers-hydrogel scaffold for controlled non-viral drug/gene delivery to direct axon regeneration in spinal cord injury treatment. *Sci. Rep.* **2017**, *7*, 42212.

[87] Salerno, A.; Iannace, S.; Netti, P. A. Graded biomimetic osteochondral scaffold prepared via CO_2 foaming and micronized NaCl leaching. *Mater. Lett.* **2012**, *82*, 137–140.

[88] Wang, Y. Z.; Xu, R.; Luo, G. X.; Lei, Q.; Shu, Q.; Yao, Z. H.; Li, H. S.; Zhou, J. Y.; Tan, J. L.; Yang, S. et al. Biomimetic fibroblast-loaded artificial dermis with "sandwich" structure and designed gradient pore sizes promotes wound healing by favoring granulation tissue formation and wound re-epithelialization. *Acta Biomater.* **2016**, *30*, 246–257.

[89] Huang, L.; Huang, J. W.; Shao, H. L.; Hu, X. C.; Cao, C. B.; Fan, S. N.; Song, L. J.; Zhang, Y. P. Silk scaffolds with gradient pore structure and improved cell infiltration performance. *Mater. Sci. Eng.: C* **2019**, *94*, 179–189.

[90] He, M.; Wang, Q.; Xie, L.; Wu, H.; Zhao, W. F.; Tian, W. D. Hierarchically multi-functionalized graded membrane with enhanced bone regeneration and self-defensive antibacterial characteristics for guided bone regeneration. *Chem. Eng. J.* **2020**, *398*, 125542.

[91] Bottino, M. C.; Thomas, V.; Janowski, G. M. A novel spatially designed and functionally graded electrospun membrane for periodontal regeneration. *Acta Biomater.* **2011**, *7*, 216–224.

[92] Wu, T. T.; Ding, M. Z.; Shi, C. P.; Qiao, Y. Q.; Wang, P. P.; Qiao, R. R.; Wang, X. C.; Zhong, J. Resorbable polymer electrospun nanofibers: History, shapes and application for tissue engineering. *Chin. Chem. Lett.* **2020**, *31*, 617–625.

[93] Oh, S. H.; Park, I. K.; Kim, J. M.; Lee, J. H. *In vitro* and *in vivo* characteristics of PCL scaffolds with pore size gradient fabricated by a centrifugation method. *Biomaterials* **2007**, *28*, 1664–1671.

[94] Lowery, J. L.; Datta, N.; Rutledge, G. C. Effect of fiber diameter, pore size and seeding method on growth of human dermal fibroblasts in electrospun poly(ε-caprolactone) fibrous mats. *Biomaterials* **2010**, *31*, 491–504.

[95] Mbundi, L.; González-Pérez, M.; González-Pérez, F.; Juanes-Gusano, D.; Rodríguez-Cabello, J. Trends in the development of tailored elastin-like recombinamer–based porous biomaterials for soft and hard tissue applications. *Front. Mater.* **2021**, *7*, 601795.

[96] Walser, J.; Stok, K. S.; Caversaccio, M. D.; Ferguson, S. J. Direct electrospinning of 3D auricle-shaped scaffolds for tissue engineering applications. *Biofabrication* **2016**, *8*, 025007.

[97] Eichholz, K. F.; Hoey, D. A. Mediating human stem cell behaviour via defined fibrous architectures by melt electrospinning writing. *Acta Biomater.* **2018**, *75*, 140–151.

[98] He, F. L.; Li, D. W.; He, J.; Liu, Y. Y.; Ahmad, F.; Liu, Y. L.; Deng, X. D.; Ye, Y. J.; Yin, D. C. A novel layer-structured scaffold with large pore sizes suitable for 3D cell culture prepared by near-field electrospinning. *Mater. Sci. Eng.: C* **2018**, *86*, 18–27.

[99] Aghajanpoor, M.; Hashemi-Najafabadi, S.; Baghaban- Eslaminejad, M.; Bagheri, F.; Mohammad Mousavi, S.; Azam Sayyahpour, F. The effect of increasing the pore size of nanofibrous scaffolds on the osteogenic cell culture using a combination of sacrificial agent electrospinning and ultrasonication. *J. Biomed. Mater. Res. Part A* **2017**, *105*, 1887–1899.

[100] Yuan, L.; Li, X. Y.; Ge, L. M.; Jia, X. Q.; Lei, J. F.; Mu, C. D.; Li, D. F. Emulsion template method for the fabrication of gelatin-based scaffold with a controllable pore structure. *ACS Appl. Mater. Interfaces* **2019**, *11*, 269–277.

[101] Park, H. J.; Lee, O. J.; Lee, M. C.; Moon, B. M.; Ju, H. W.; Lee, J. M.; Kim, J. H.; Kim, D. W.; Park, C. H. Fabrication of 3D porous silk scaffolds by particulate (salt/sucrose) leaching for bone tissue reconstruction. *Int. J. Biol. Macromol.* **2015**, *78*, 215–223.

[102] Refifi, J.; Oudadesse, H.; Merdrignac-Conanec, O.; El Feki, H.; Lefeuvre, B. Salt leaching using powder (SLUP) process for glass/chitosan scaffold elaboration for biomaterial applications. *J. Aust. Ceram. Soc.* **2020**, *56*, 1167–1178.

[103] Coogan, K. R.; Stone, P. T.; Sempertegui, N. D.; Rao, S. S. Fabrication of micro-porous hyaluronic acid hydrogels through salt leaching. *Eur. Polym. J.* **2020**, *135*, 109870.

[104] Lin, J. Y.; Ding, B.; Yu, J. Y.; Hsieh, Y. Direct fabrication of highly nanoporous polystyrene fibers via electrospinning. *ACS Appl. Mater. Interfaces* **2010**, *2*, 521–528.

[105] Cheng, T. T.; Li, S. Q.; Xu, L.; Ahmed, A. Controllable preparation and formation mechanism of nanofiber membranes with large pore sizes using a modified electrospinning. *Mater. Des.* **2019**, *178*, 107867.

[106] Watson, N. J.; Johal, R. K.; Glover, Z.; Reinwald, Y.; White, L. J.; Ghaemmaghami, A. M.; Morgan, S. P.; Rose, F. R. A. J.; Povey, M. J. W.; Parker, N. G. Post-processing of polymer foam tissue scaffolds with high power ultrasound: A route to increased pore interconnectivity, pore size and fluid transport. *Mater. Sci. Eng.: C* **2013**, *33*, 4825–4832.

[107] Lee, J. B.; Jeong, S. I.; Bae, M. S.; Yang, D. H.; Heo, D. N.; Kim, C. H.; Alsberg, E.; Kwon, I. K. Highly porous electrospun nanofibers enhanced by ultrasonication for improved cellular infiltration. *Tissue Eng. Part A* **2011**, *17*, 2695–2702.

[108] Ekaputra, A. K.; Prestwich, G. D.; Cool, S. M.; Hutmacher, D. W. Combining electrospun scaffolds with electrosprayed hydrogels leads to three-dimensional cellularization of hybrid constructs. *Biomacromolecules* **2008**, *9*, 2097–2103.

[109] Zhu, X. L.; Cui, W. G.; Li, X. H.; Jin, Y. Electrospun fibrous mats with high porosity as potential scaffolds for skin tissue engineering. *Biomacromolecules* **2008**, *9*, 1795–1801.

[110] Sheikh, F. A.; Ju, H. W.; Lee, J. M.; Moon, B. M.; Park, H. J.; Lee, O. J.; Kim, J. H.; Kim, D. K.; Park, C. H. 3D electrospun silk fibroin nanofibers for fabrication of artificial skin. *Nanomedicine: Nanotechnol., Biol. Med.* **2015**, *11*, 681–691.

[111] Simonet, M.; Schneider, O. D.; Neuenschwander, P.; Stark, W. J. Ultraporous 3D polymer meshes by low-temperature electrospinning: Use of ice crystals as a removable void template. *Polym. Eng. Sci.* **2007**, *47*, 2020–2026.

[112] Leong, M. F.; Rasheed, M. Z.; Lim, T. C.; Chian, K. S. *In vitro* cell infiltration and *in vivo* cell infiltration and vascularization in a fibrous, highly porous poly(D,L-lactide) scaffold fabricated by cryogenic electrospinning technique. *J. Biomed. Mater. Res. Part A* **2009**, *91A*, 231–240.

[113] Ko, J.; Kan, D. Y.; Jun, M. B. G. Combining melt electrospinning and particulate leaching for fabrication of porous microfibers. *Manuf. Lett.* **2015**, *3*, 5–8.

[114] Pham, O. P.; Sharma, U.; Mikos, A. G. Electrospun Poly(ε-caprolactone) microfiber and multilayer nanofiber/microfiber scaffolds: Characterization of scaffolds and measurement of cellular infiltration. *Macromolecules* **2006**, *7*, 2796–2805.
[115] Larrondo, L.; St. John Manley, R. Electrostatic fiber spinning from polymer melts. I. Experimental observations on fiber formation and properties. *J. Polym. Sci.: Polym. Phys. Ed.* **1981**, *19*, 909–920.
[116] Brown, T. D.; Dalton, P. D.; Hutmacher, D. W. Melt electrospinning today: An opportune time for an emerging polymer process. *Prog. Polym. Sci.* **2016**, *56*, 116–166.
[117] Wunner, F. M.; Wille, M. L.; Noonan, T. G.; Bas, O.; Dalton, P. D.; De-Juan-Pardo, E. M.; Hutmacher, D. W. Melt electrospinning writing of highly ordered large volume scaffold architectures. *Adv. Mate.* **2018**, *30*, 1706570.
[118] Rothrauff, B. B.; Lauro, B. B.; Yang, G.; Debski, R. E.; Musahl, V.; Tuan, R. S. Braided and stacked electrospun nanofibrous scaffolds for tendon and ligament tissue engineering. *Tissue Eng. Part A* **2017**, *23*, 378–389.
[119] Park, S. H.; Kim, M. S.; Lee, B.; Park, J. H.; Lee, H. J.; Lee, N. K.; Jeon, N. L.; Suh, K. Y. Creation of a hybrid scaffold with dual configuration of aligned and random electrospun fibers. *ACS Appl. Mater. Interfaces* **2016**, *8*, 2826–2832.
[120] Shim, I. K.; Suh, W. H.; Lee, S. Y.; Lee, S. H.; Heo, S. J.; Lee, M. C.; Lee, S. J. Chitosan nano-/microfibrous double-layered membrane with rolled-up three-dimensional structures for chondrocyte cultivation. *J. Biomed. Mater. Res. Part A* **2009**, *90A*, 595–602.
[121] Zhou, J.; Cao, C. B.; Ma, X. L. A novel three-dimensional tubular scaffold prepared from silk fibroin by electrospinning. *Int. J. Biol. Macromol.* **2009**, *45*, 504–510.
[122] Joung, D.; Lavoie, N. S.; Guo, S. Z.; Park, S. H.; Parr, A. M.; McAlpine, M. C. 3D printed neural regeneration devices. *Adv. Funct. Mater.* **2020**, *30*, 1906237.
[123] Chen, W. M.; Xu, Y.; Li, Y. Q.; Jia, L. T.; Mo, X. M.; Jiang, G. N.; Zhou, G. D. 3D printing electrospinning fiber-reinforced decellularized extracellular matrix for cartilage regeneration. *Chem. Eng. J.* **2020**, *382*, 122986.
[124] Chen, T. T.; Bakhshi, H.; Liu, L.; Ji, J.; Agarwal, S. Combining 3D printing with electrospinning for rapid response and enhanced designability of hydrogel actuators. *Adv. Funct. Mater.* **2018**, *28*, 1800514.
[125] Eom, S.; Park, S. M.; Hong, H.; Kwon, J.; Oh, S. R.; Kim, J.; Kim, D. S. Hydrogel-assisted electrospinning for fabrication of a 3D complex tailored nanofiber macrostructure. *ACS Appl. Mater. Interfaces* **2020**, *12*, 51212–51224.
[126] Lee, J. S.; Chae, S.; Yoon, D.; Yoon, D.; Chun, W.; Kim, G. H. Angiogenic factors secreted from human ASC spheroids entrapped in an alginate-based hierarchical structure via combined 3D printing/electrospinning system. *Biofabrication* **2020**, *12*, 045028.
[127] Sun, D. H.; Chang, C.; Li, S.; Lin, L. W. Near-field electrospinning. *Nano Lett.* **2006**, *6*, 839–842.
[128] Su, Y. C.; Qiu, T.; Song, W.; Han, X. J.; Sun, M. M.; Wang, Z.; Xie, H.; Dong, M. D.; Chen, M. L. Melt electrospinning writing of magnetic microrobots. *Adv. Sci.* **2021**, *8*, 2003177.
[129] Brown, T. D.; Dalton, P. D.; Hutmacher, D. W. Direct writing by way of melt electrospinning. *Adv. Mater.* **2011**, *23*, 5651–5657.
[130] He, J. K.; Xu, F. Y.; Cao, Y.; Liu, Y. X.; Li, D. C. Towards microscale electrohydrodynamic three-dimensional printing. *J. Phys. D: Appl. Phys.* **2016**, *49*, 055504.
[131] Park, Y. S.; Kim, J.; Oh, J. M.; Park, S.; Cho, S.; Ko, H.; Cho, Y. K. Near-field electrospinning for three-dimensional stacked nano-architectures with high aspect ratios. *Nano Lett.* **2020**, *20*, 441–448.
[132] Rahmati, M.; Mills, D. K.; Urbanska, A. M.; Saeb, M. R.; Venugopal, J. R.; Ramakrishna, S.; Mozafari, M. Electrospinning for tissue engineering applications. *Prog. Mater. Sci.* **2021**, *117*, 100721.
[133] Wu, T.; Huang, C.; Li, D. W.; Yin, A. L.; Liu, W.; Wang, J.; Chen, J. F.; Ei-Hamshary, H.; Al-Deyab, S. S.; Mo, X. A multi-layered vascular scaffold with symmetrical structure by bi-directional gradient electrospinning. *Colloids Surf. B: Biointerf.* **2015**, *133*, 179–188.
[134] Lu, S. T.; Fan, X. C.; Wang, H. N.; Zhao, Y. L.; Zhao, W. C.; Li, M. Z.; Lv, R. Y.; Wang, T.; Sun, T. D. Synthesis of gelatin-based dual-targeted nanoparticles of betulinic acid for antitumor therapy. *ACS Appl. Bio Mater.* **2020**, *3*, 3518–3525.
[135] Ugarte-Berzal, E.; Vandooren, J.; Bailón, E.; Opdenakker, G.; García-Pardo, A. Inhibition of MMP-9-dependent degradation of gelatin, but not other MMP-9 substrates, by the MMP-9 hemopexin domain blades 1 and 4. *J. Biol. Chem.* **2016**, *291*, 11751–11760.
[136] Zhao, X.; Sun, X. M.; Yildirimer, L.; Lang, Q.; Lin, Z. Y.; Zheng, R.; Zhang, Y. G.; Cui, W. G.; Annabi, N.; Khademhosseini, A. Cell infiltrative hydrogel fibrous scaffolds for accelerated wound healing. *Acta Biomater.* **2017**, *49*, 66–77.
[137] Wen, P.; Zong, M. H.; Linhardt, R. J.; Feng, K.; Wu, H. Electrospinning: A novel nano-encapsulation approach for bioactive compounds. *Trends Food Sci. Technol.* **2017**, *70*, 56–68.
[138] Hou, Z. Y.; Li, X. J.; Li, C. X.; Dai, Y. L.; Ma, P. A.; Zhang, X.; Kang, X. J.; Cheng, Z. Y.; Lin, J. Electrospun upconversion composite fibers as dual drugs delivery system with individual release properties. *Langmuir* **2013**, *29*, 9473–9482.
[139] Zhang, Z. Y.; Liu, S.; Qi, Y. X.; Zhou, D. F.; Xie, Z. G.; Jing, X. B.; Chen, X. S.; Huang, Y. B. Time-programmed DCA and oxaliplatin release by multilayered nanofiber mats in prevention of local cancer recurrence following surgery. *J. Control. Release* **2016**, *235*, 125–133.
[140] Honarbakhsh, S.; Guenther, R. H.; Willoughby, J. A.; Lommel, S. A.; Pourdeyhimi, B. Polymeric systems incorporating plant viral nanoparticles for tailored release of therapeutics. *Adv. Healthc. Mater.* **2013**, *2*, 1001–1007.
[141] Han, J. P.; Liang, C. Y.; Cui, Y. C.; Xiong, L. K.; Guo, X. C.; Yuan, X. Y.; Yang, D. Y. Encapsulating microorganisms inside electrospun microfibers as a living material enables room-temperature storage of microorganisms. *ACS Appl. Mater. Interfaces* **2018**, *10*, 38799–38806.
[142] Zussman, E. Encapsulation of cells within electrospun fibers. *Polym. Adv. Technol.* **2011**, *22*, 366–371.
[143] Letnik, I.; Avrahami, R.; Rokem, J. S.; Greiner, A.; Zussman, E.; Greenblatt, C. Living composites of electrospun yeast cells for bioremediation and ethanol production. *Biomacromolecules* **2015**, *16*, 3322–3328.
[144] Bao, Z. T.; Xian, C. H.; Yuan, Q. J.; Liu, G. T.; Wu, J. Natural polymer-based hydrogels with enhanced mechanical performances: Preparation, structure, and property. *Adv. Healthc. Mater.* **2019**, *8*, 1900670.
[145] Lai, H. J.; Kuan, C. H.; Wu, H. C.; Tsai, J. C.; Chen, T. M.; Hsieh, D. J.; Wang, T. W. Tailored design of electrospun composite nanofibers with staged release of multiple angiogenic growth factors for chronic wound healing. *Acta Biomater.* **2014**, *10*, 4156–4166.
[146] Yau, W. W. Y.; Long, H. Y.; Gauthier, N. C.; Chan, J. K. Y.; Chew, S. Y. The effects of nanofiber diameter and orientation on siRNA uptake and gene silencing. *Biomaterials* **2015**, *37*, 94–106.
[147] Zhou, F.; Jia, X. L.; Yang, Y.; Yang, Q. M.; Gao, C.; Hu, S. L.; Zhao, Y. H.; Fan, Y. B.; Yuan, X. Y. Nanofiber-mediated microRNA-126 delivery to vascular endothelial cells for blood vessel regeneration. *Acta Biomater.* **2016**, *43*, 303–313.
[148] Liao, I. C.; Chen, S. L.; Liu, J. B.; Leong, K. W. Sustained viral gene delivery through core-shell fibers. *J. Control. Release* **2009**, *139*, 48–55.
[149] Wang, X. C.; Lv, F.; Li, T.; Han, Y. M.; Yi, Z. F.; Liu, M. Y.; Chang, J.; Wu, C. T. Electrospun micropatterned nanocomposites incorporated with Cu_2S nanoflowers for skin tumor therapy and wound healing. *ACS Nano* **2017**, *11*, 11337–11349.
[150] Cheng, G.; Yin, C. C.; Tu, H.; Jiang, S.; Wang, Q.; Zhou, X.; Xing, X.; Xie, C. Y.; Shi, X. W.; Du, Y. M. et al. Controlled Co-delivery of growth factors through layer-by-layer assembly of core–shell nanofibers for improving bone regeneration. *ACS Nano* **2019**, *13*, 6372–6382.
[151] Chen, W. M.; Chen, S.; Morsi, Y.; El-Hamshary, H.; El-Newhy, M.; Fan, C. Y.; Mo, X. M. Superabsorbent 3D scaffold based on electrospun nanofibers for cartilage tissue engineering. *ACS Appl. Mater. Interfaces* **2016**, *8*, 24415–24425.

[152] Liu, Y.; Zhou, S. Y.; Gao, Y. L.; Zhai, Y. L. Electrospun nanofibers as a wound dressing for treating diabetic foot ulcer. *Asian J. Pharm. Sci*. **2019**, *14*, 130–143.
[153] Yan, X.; Yu, M.; Ramakrishna, S.; Russell, S. J.; Long, Y. Z. Advances in portable electrospinning devices for *in situ* delivery of personalized wound care. *Nanoscale* **2019**, *11*, 19166–19178.
[154] Nicholas, M. N.; Jeschke, M. G.; Amini-Nik, S. Cellularized bilayer pullulan-gelatin hydrogel for skin regeneration. *Tissue Eng. Part A* **2016**, *22*, 754–764.
[155] Dai, X. Z.; Kathiria, K.; Huang, Y. C. Electrospun fiber scaffolds of poly (glycerol-dodecanedioate) and its gelatin blended polymers for soft tissue engineering. *Biofabrication* **2014**, *6*, 035005.
[156] Millán-Rivero, J. E.; Martínez, C. M.; Romecín, P. A.; Aznar-Cervantes, S. D.; Carpes-Ruiz, M.; Cenis, J. L.; Moraleda, J. M.; Atucha, N. M.; García-Bernal, D. Silk fibroin scaffolds seeded with Wharton's jelly mesenchymal stem cells enhance re-epithelialization and reduce formation of scar tissue after cutaneous wound healing. *Stem Cell Res. Ther*. **2019**, *10*, 126.
[157] Ju, Y. M.; Choi, J. S.; Atala, A.; Yoo, J. J.; Lee, S. J. Bilayered scaffold for engineering cellularized blood vessels. *Biomaterials* **2010**, *31*, 4313–4321.
[158] Norouzi, S. K.; Shamloo, A. Bilayered heparinized vascular graft fabricated by combining electrospinning and freeze drying methods. *Mater. Sci. Eng.: C* **2019**, *94*, 1067–1076.
[159] Ye, L.; Cao, J.; Chen, L. M.; Geng, X.; Zhang, A. Y.; Guo, L. R.; Gu, Y. Q.; Feng, Z. G. The fabrication of double layer tubular vascular tissue engineering scaffold via coaxial electrospinning and its 3D cell coculture. *J. Biomed. Mater. Res. Part A* **2015**, *103*, 3863–3871.
[160] Dejob, L.; Toury, B.; Tadier, S.; Grémillard, L.; Gaillard, C.; Salles, V. Electrospinning of *in situ* synthesized silica-based and calcium phosphate bioceramics for applications in bone tissue engineering: A review. *Acta Biomater*. **2021**, *123*, 123–153.
[161] Szurkowska, K.; Kolmas, J. Hydroxyapatites enriched in silicon – Bioceramic materials for biomedical and pharmaceutical applications. *Prog. Nat. Sci.: Mater. Int*. **2017**, *27*, 401–409.
[162] Bas, O.; De-Juan-Pardo, E. M.; Meinert, C.; D'Angella, D.; Baldwin, J. G.; Bray, L. J.; Wellard, R. M.; Kollmannsberger, S.; Rank, E.; Werner, C. et al. Biofabricated soft network composites for cartilage tissue engineering. *Biofabrication* **2017**, *9*, 025014.
[163] Bas, O.; Lucarotti, S.; Angella, D. D.; Castro, N. J.; Meinert, C.; Wunner, F. M.; Rank, E.; Vozzi, G.; Klein, T. J.; Catelas, I. et al. Rational design and fabrication of multiphasic soft network composites for tissue engineering articular cartilage: A numerical model-based approach. *Chem. Eng. J*. **2018**, *340*, 15–23.
[164] Chen, H. L.; de Botelho Ferreira Braga Malheiro, A.; van Blitterswijk, C.; Mota, C.; Wieringa, P. A.; Moroni, L. Direct writing electrospinning of scaffolds with multidimensional fiber architecture for hierarchical tissue engineering. *ACS Appl. Mater. Interfaces* **2017**, *9*, 38187–38200.
[165] Ghosh, S. K.; Adhikary, P.; Jana, S.; Biswas, A.; Sencadas, V.; Gupta, S. D.; Tudu, B.; Mandal, D. Electrospun gelatin nanofiber based self-powered bio-*e*-skin for health care monitoring. *Nano Energy* **2017**, *36*, 166–175.
[166] Zhang, J.; Zhao, Y. T.; Hu, P. Y.; Liu, J. J.; Liu, X. F.; Hu, M. Z.; Cui, Z. M.; Wang, N.; Niu, Z. Y.; Xiang, H. F. et al. Laparoscopic electrospinning for *in situ* hemostasis in minimally invasive operation. *Chem. Eng. J*. **2020**, *395*, 125089.
[167] Lee, J. K. Y.; Chen, N.; Peng, S. J.; Li, L. L.; Tian, L. L.; Thakor, N.; Ramakrishna, S. Polymer-based composites by electrospinning: Preparation & functionalization with nanocarbons. *Prog. Polym. Sci*. **2018**, *86*, 40–84.
[168] Sonseca, A.; Sahay, R.; Stepien, K.; Bukala, J.; Wcislek, A.; McClain, A.; Sobolewski, P.; Sui, X. M.; Puskas, J. E.; Kohn, J. et al. Architectured helically coiled scaffolds from elastomeric poly(butylene succinate) (PBS) copolyester via wet electrospinning. *Mater. Sci. Eng.: C* **2020**, *108*, 110505.
[169] Allafchian, A.; Hosseini, H.; Ghoreishi, S. M. Electrospinning of PVA-carboxymethyl cellulose nanofibers for flufenamic acid drug delivery. *Int. J. Biol. Macromol*. **2020**, *163*, 1780–1786.
[170] Choi, E. S.; Kim, H. C.; Muthoka, R. M.; Panicker, P. S.; Agumba, D. O.; Kim, J. Aligned cellulose nanofiber composite made with electrospinning of cellulose nanofiber - Polyvinyl alcohol and its vibration energy harvesting. *Compos. Sci. Technol*. **2021**, *209*, 108795.
[171] Yao, T. Y.; Chen, H. L.; Samal, P.; Giselbrecht, S.; Baker, M. B.; Moroni, L. Self-assembly of electrospun nanofibers into gradient honeycomb structures. *Mater. Des*. **2019**, *168*, 107614.
[172] Xie, S.; Zeng, Y. C. Effects of electric field on multineedle electrospinning: Experiment and simulation study. *Ind. Eng. Chem. Res*. **2012**, *51*, 5336–5345.
[173] Yang, Y.; Jia, Z. D.; Li, Q.; Hou, L.; Liu, J. N.; Wang, L. M.; Guan, Z. C.; Zahn, M. A shield ring enhanced equilateral hexagon distributed multi-needle electrospinning spinneret. *IEEE Trans. Dielectr. Electr. Insul*. **2010**, *17*, 1592–1601.
[174] Zhang, X. Q.; Wu, J.; Wang, J. T.; Zhang, J.; Yang, Q. Q.; Fu, Y. Y.; Xie, Z. Y. Highly conductive PEDOT:PSS transparent electrode prepared by a post-spin-rinsing method for efficient ITO-free polymer solar cells. *Solar Energy Mater. Solar Cells* **2016**, *144*, 143–149.